Human Molecular Genetics, 2006, Vol. 15, No. 11 ***1894–1913***
doi:10.1093/hmg/ddl112
Advance Access published on April 27, 2006

The role of PI3K/AKT, MAPK/ERK and NFκβ signalling in the maintenance of human embryonic stem cell pluripotency and viability highlighted by transcriptional profiling and functional analysis

Lyle Armstrong[1,2,†], Owen Hughes[1,2,†], Sun Yung[1,2], Louise Hyslop[1,2], Rebecca Stewart[1,2], Ilka Wappler[1,2], Heiko Peters[1,2], Theresia Walter[1,2], Petra Stojkovic[1,2,‡], Jerome Evans[2], Miodrag Stojkovic[1,2,‡] and Majlinda Lako[1,2,*]

[1]Centre for Stem Cell Biology and [2]Developmental Genetics, Institute of Human Genetics, University of Newcastle, Newcastle upon Tyne, UK

Received January 16, 2006; Revised March 11, 2006; Accepted April 11, 2006

Understanding the molecular mechanism by which pluripotency is maintained in human embryonic stem cells (hESC) is important for the development of improved methods to derive, culture and differentiate these into cells of potential therapeutic use. Large-scale transcriptional comparison of the hES-NCL1 line derived from a day 8 embryo with H1 line derived from a day 5 embryo (WiCell Inc.) showed that only 0.52% of the transcripts analysed varied significantly between the two cell lines. This is within the variability range that has been reported when hESC derived from days 5–6 embryos have been compared with each other. This implies that transcriptional differences between the cell lines are likely to reflect their genetic profile rather than the embryonic stage from which they were derived. Bioinformatic analysis of expression changes observed when these cells were induced to differentiate as embryoid bodies suggested that quite a few of the downregulated genes were components of signal transduction networks. Subsequent analysis using western blotting, flow cytometry and antibody arrays implicated components of the PI3K/AKT kinase, MAPK/ERK and NFκβ pathways and confirmed that these components are decreased upon differentiation. Disruption of these pathways in isolation using specific inhibitors resulted in loss of pluripotency and/or loss of viability suggesting the importance of such signalling pathways in embryonic stem cell maintenance.

INTRODUCTION

Human embryonic stem cells (hESC) hold great promise for understanding early human embryonic development and generating clinically useful cell lines (1,2). In view of this a great deal of effort is focused on experiments aimed at improving culture conditions (3), generating new hESC lines suitable for clinical purposes (4), genetic manipulation (5,6) and differentiation regimes to produce human cells suitable for transplantation and drug testing (7,8). To date, more than

*To whom correspondence should be addressed at: Centre for Stem Cell Biology and Developmental Genetics, Institute of Human Genetics, University of Newcastle upon Tyne, International Centre for Life, Central Parkways, Newcastle upon Tyne NE1 3BZ, UK. Tel: +44 1912418688; Fax: +44 1912418666; Email: majlinda.lako@ncl.ac.uk
†The authors wish it to be known that, in their opinion, the first two authors should be regarded as joint First Authors.
‡Present address: Centro de Investigación Príncipe Felipe, Valencia, Spain.

300 hESC lines have been derived worldwide; however, only a handful of these have been extensively characterized using large-scale transcriptomic approaches. These techniques have shown that similar to murine ESC (mESC), hESC express some of the classical markers of pluripotent stem cell lines such as OCT4, NANOG, alkaline phosphatase (AP) and high levels of telomerase activity (1). However, there are many notable differences between human and mouse ESC in both morphological and behavioral characteristics such as colony thickness, shape and population doubling time (9). The expression of cell surface marker proteins differs considerably (10) and large-scale transcriptional profiling studies undertaken by a number of groups reveal that ~10% of the genes showing significant expression changes between mouse and human ESC are involved in oxidative phosphorylation, suggesting that mESC have a higher ability to generate ATP and higher metabolic rate powered by mitochondrial oxidation (11). Although leukaemia inhibitory factor (LIF) modulated through gp130 signalling and the JAK/STAT pathway is sufficient for the maintenance of undifferentiated mESC, it cannot prevent the spontaneous differentiation of hESC (12). In addition, hESC unlike mESC can spontaneously differentiate to trophectoderm (13). These differences between mouse and human cells suggest that although the same pluripotentiality genes are expressed in both mouse and human ESC, their function and downstream signalling pathways may differ between the two species. This highlights the importance and necessity of studying signalling pathways that underline the maintenance of pluripotency and viability in hESC given the potential importance of stem cell therapies in therapeutic medicine.

Recent publications detailing transcriptional profiling of several hESC lines (14–23) have shown that there are common genes expressed in several cell lines. However, each cell line possesses a unique expression signature which may reflect either the genetic profile of the embryo from which they have been derived or the differences in conditions used either for the derivation, culture or cryopreservation of cell lines in different laboratories (22,23). The differences in gene expression might also be a function of the developmental stage of the embryo from which the hESC lines are derived; however, this hypothesis has been difficult to test because the majority of the hESC lines were derived from days 5–6 blastocysts. More recently, derivation of cell lines from morulae has been described (24), and 2 years ago, our group was able to isolate a new hESC line, hES-NCL1 from day 8 human embryos using a novel three-step culture condition approach (25). This cell line gives us a unique ability to assess whether the developmental stage of the embryo affects the transcriptional profile of the hESC lines. In this manuscript, we report for the first time that the developmental stage of the embryo does not enhance the transcriptional differences already reported between different cell lines and therefore these are more likely to be due to genetic profile of the embryo from which they are derived. We also highlight three signalling pathways, namely PI3K/AKT, RAS/MAPK and NFκβ, and indicate that they are crucial for the maintenance of pluripotency and/or viability in hESC.

RESULTS

hES-NCL1 cell line shows similar phenotypic and transcriptional characteristics to H1 cells

Recently, we reported the derivation of a new hESC line, hES-NCL1, from day 8 embryos, using novel three-step culture conditions (25). The majority of the hESC lines reported to date have been derived from days 5 and 6 embryos. In view of this, we set out to compare our cell line hES-NCL1 with the H1 line available from WiCell Inc. (Madison, USA) and to determine whether these cells derived from day 8 embryos showed any phenotypic or significant transcriptional difference to cells derived from earlier embryos (such as the H1 line). Both of these cell lines have been extensively characterized *in vitro* and shown to contribute to teratoma formation *in vivo* (1,25). We cultured the two cell lines under the same conditions (see Materials and Methods) and by the same investigator continuously up to passage 70. We first examined the expression of cell surface markers (TRA-1-60, TRA-1-81, SSEA-3, 4, 1, CD117 and CD135) by flow cytometry at passages 38 (Fig. 1A), 56 (data not shown) and 70. In all cases, we observed very similar marker expression for both cell lines. No gross karyotypic abnormalities were found up to 70 continuous passages in culture (Fig. 1B). Both of the cell lines expressed markers such as *OCT4*, *NANOG*, *REX1* and *TERT* at both passages 38 (data not shown) and 70 (Fig. 1C) as shown by the reverse transcription assay. As this method is only semi-quantitative and does not reflect properly the levels of gene expression between the two cell lines, we investigated their relative expression using microarray technology as outlined in Expression profiling of hES-NCL1 and H1: comparison with other hESC lines. This indicated that there was no significant difference in the expression levels of *NANOG*, *OCT4*, *TERT* and *REX1* between the two cell lines (Fig. 1D; in all cases, $P > 0.5$). This result was confirmed by real-time reverse transcription (RT)–PCR analysis (data not shown).

To assess the growth rate of the two cell lines, hESC colonies were disrupted to single cells by digestion with accutase, which results in much higher cell viability compared with trypsin digestion (our own unpublished data). Fifty thousand cells were plated in triplicate on fresh mitotically inactivated mouse embryonic fibroblasts and allowed to grow for 5 days before being subjected to the digestion procedure and counted again. This was repeated for five passages and the results indicate that the average population doubling time for the hES-NCL1 line was 43.5 h and that for the H1 line was 44.2 h.

To assess the degree of variability in differentiation capacity, we removed colonies of both hESC lines from the feeder cells and cultured them in suspension as embryoid bodies (EBs) for up to 15 days. Differentiation was confirmed by flow cytometry for the hESC-specific cell surface marker, TRA-1-60 which showed significant downregulation during the differentiation of hESC (74% of the hESC stained with TRA-1-60) to EBs (6.05 and 4.11% of the cells remained TRA-160-positive after 7 and 14 days of differentiation, respectively; data are presented as an average of both cell lines). Samples of cells were removed at days 0, 5, 10 and 15 and subjected to quantitative real-time RT–PCR for

A

Antibody	hES-NCL1	H1
TRA-1-60	74.4 ± 1.6 74.5 ± 1.9	73.6 ± 2.6 75.9 ± 2.8
TRA-1-81	73.9 ± 0.9 72.5 ± 4.6	74.3 ± 2.1 75.4 ± 3.1
SSEA-4	56.6 ± 1.3 58.6 ± 3.9	60.3 ± 2.2 63.3 ± 3.3
SSEA-1	19.5 ± 3.5 19.8 ± 2.3	20.5 ± 4.2 19.6 ± 2.8
SSEA-3	63.7±1.7 62.8±5.1	66.1 ± 3.4 62.2 ± 2.2
CD135	29.1 ± 3.4 35.6 ± 4.3	27.8 ± 3.2 33.4 ± 4.5
CD117	19.3 ± 0.8 25.1 ± 4.5	24.5 ± 1.6 27.8 ± 2.1

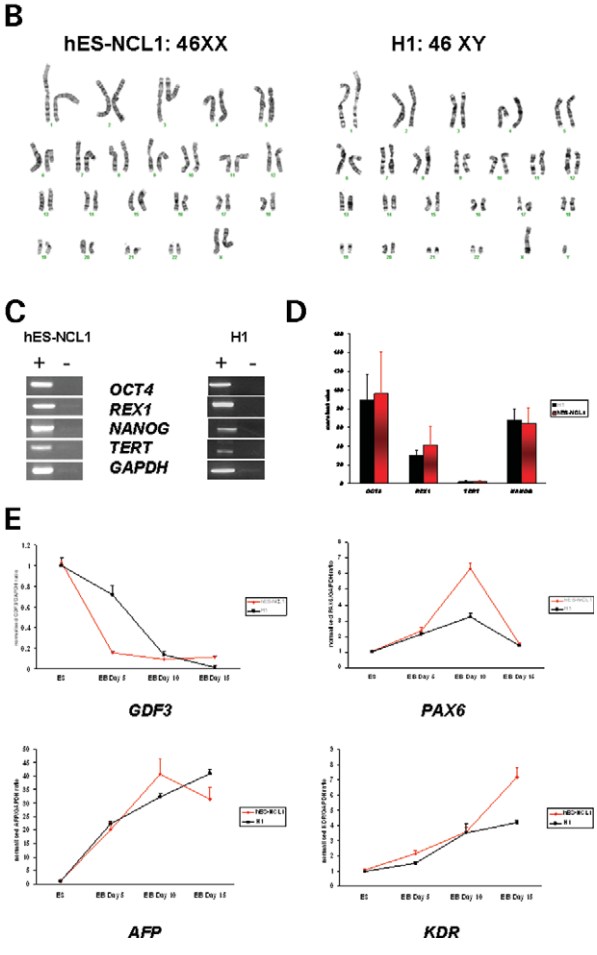

Figure 1. Phenotypic and transcriptional comparison of the hES-NCL1 line with H1. (**A**) Cell surface staining of the two hESC lines at passage 38 (shown in black) and at passage 70 (shown in red). The data represent the mean ± SEM performed on three independent measurements. (**B**) Karyotypic analysis of the two hESC lines at passage 70. (**C**) RT–PCR analysis of the two hESC lines for the expression of *OCT4, REX1*, *NANOG* and *TERT*. *GAPDH* is used as a normalizing control. '+' indicates the presence of reverse transcriptase and '−' the lack of the enzyme. (**D**) Expression analysis of *NANOG*, *OCT4*, *REX1* and *TERT* in hES-NCL1 and H1. The data are plotted as average of three normalized ratios obtained after hybridization of three separate hES-NCL1 and H1 samples to U133 Plus 2.0 array (Affymetrix). (**E**) Real-time RT–PCR analysis for pluripotency markers (*GDF3*), endoderm markers (*AFP*), mesoderm markers (*KDR*) and ectodermal marker (*PAX6*) during differentiation of hESC to EBs. For each gene, the value for the hESC was set to 1 and all other values were calculated with respect to this.

markers of pluripotency (*GDF3*), endoderm (*AFP*), mesoderm (*KDR*) and ectoderm (*PAX6*; Fig. 1E). As reported for other cell lines (14), both lines used in the study differentiated into cells that expressed markers indicative of the three germ layers. However, there were some differences in the expression levels of the same gene between the two cell lines studies at identical time points which might indicate their preference for differentiation towards a specific lineage. Most importantly, changes in marker expression can reflect the level of spontaneous differentiation occurring at different rate in different hESC lines. Although we have tried to minimize such differences between the two cell lines (Fig. 1A), the real-time RT–PCR is a sensitive technique, and hence minor changes in the level of spontaneous differentiation can result in rather major changes in gene expression during the differentiation of these two cell lines.

Expression profiling of hES-NCL1 and H1: comparison with other hESC lines

The gene expression pattern in both cell lines was assessed by hybridization of their respective mRNA output at passages 38–45 to the human U133 Plus 2.0 array which represents a coverage of 47 000 transcripts and variants including 38 500 well-characterized human genes and ESTs. We only considered a gene to be present in each cell line if that gene received a present call in three independent samples and the detection *P*-value was less than 0.000244. Twenty-two thousand two hundred and thirty-two transcripts (47.3%) were found to be present in the H1 cell line and 21 683 transcripts (46.13%) were detected in the hES-NCL1 line. To identify genes that were present in both cell lines, a Venn diagram was drawn using Genespring (Fig. 2A) and this showed that 20 382 transcripts were present in both cell lines (43.3%), whereas 1850 (3.9%) transcripts were present in H1 but not in hES-NCL1 and 1301 (2.7%) transcripts were present in hES-NCL1 but not in H1. Abeyta *et al.* (14) reported that 52% of the total transcripts were shared by all the three cell lines they analysed (H9, HSF-1 and HSF-6) and this is slightly higher than that we have observed (43.3%); however, the differences might relate to stringency of criteria chosen because 'present and marginal' expression was included in their list, whereas 'present only' was the selection criterion in our study. Most importantly, this can be dependent on the number of cell lines being compared. To verify this, we extended our analysis to the four hESC cell lines of University of Helsinki (FES21, FES22, FES29 and FES30) and three hESC cell lines of Karolinska University (HS181, HS 235, HS237) kindly provided to us by Dr Heli Skottman (23). A comparative analysis of all nine cell lines indicated that less transcripts were shared between all of them (27.8% of total transcripts, Fig. 2B). This highlights the need to compare larger number of cell lines, especially if new ESC biomarkers are sought.

A number of groups have tried to identify genes that can be used as hESC markers (22,23). This approach has resulted in several gene lists which show increasing discrepancies from one publication to the next (22,23). The variability in the results probably reflects the differences in the technical

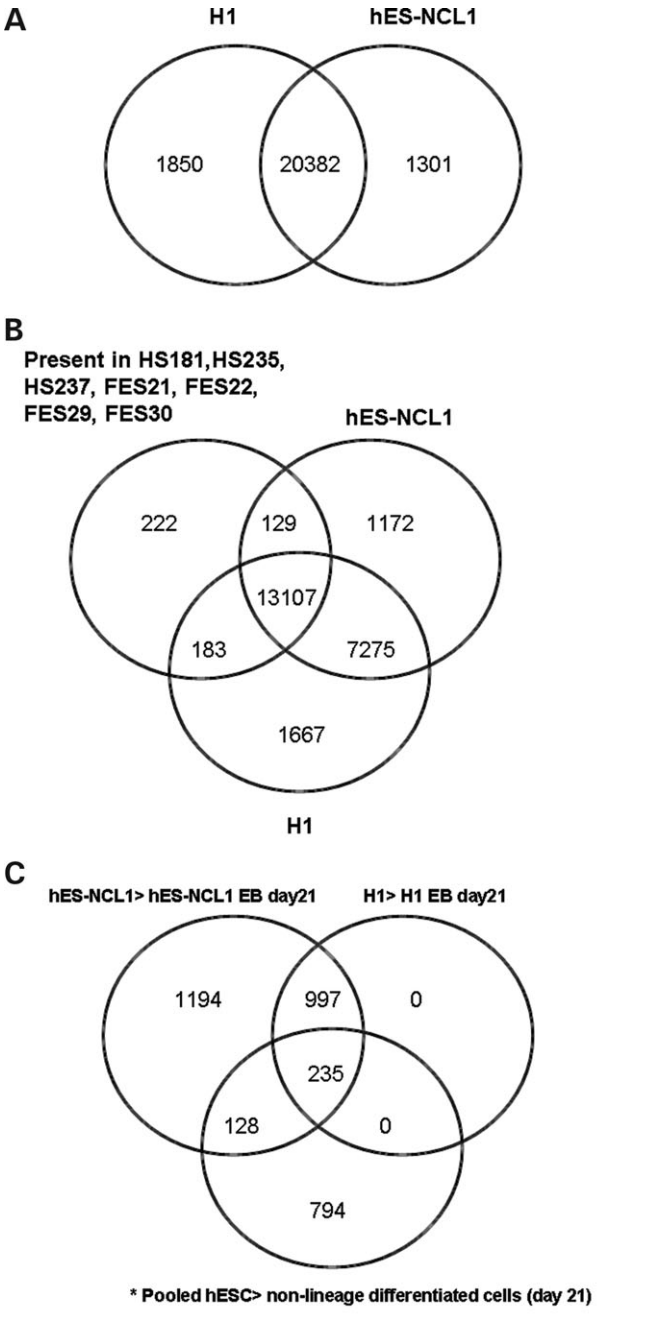

Figure 2. Expression profiling of hES-NCL1 and H1. (**A**) Venn diagram showing the transcripts present in both cell lines as well as transcripts which were specific to one of the cell lines only. (**B**) Venn diagram showing the transcripts present in all nine hESC lines (H1, hES-NCL1, FES21, FES22, FES29, FES30, HS181, HS235 and HS237). Genes that were present in FES21, FES22, FES29, FES30, HS181, HS235 and HS237 were selected by performing stepwise Venn diagram analysis for every three cell lines. (**C**) Venn diagram showing the hESC-enriched transcripts compared with non-lineage differentiated cells. The circle in the left represents the transcripts that are enriched in hES-NCL1 compared with day 21 EBs, the circle in the right represents the transcripts that are enriched in H1 compared with day 21 EBs and the circle in the bottom represents the transcripts that are enriched in pooled hESC (HS181, HS235, HS237, FES21, FES22, FES29, FES30) compared with day 21 differentiated progeny.

approach used for such large-scale expression studies (22), differences in culture conditions (23), the number of replicates and the stringency of statistical analysis as well as the availability of raw data from a large number of hESC lines (26). Because the number of transcripts shared between different cell lines is partly dependent on the number of hESC lines being compared, we hypothesized that more specific hESC biomarkers can be identified by increasing the number of cell lines being compared. To investigate this, we initially compared the H1 and hES-NCL1 lines with the differentiated progeny derived from each line to identify hESC-enriched genes. The comparison level analysis of each hESC line to non-lineage differentiated reference samples (these were differentiated progeny from hESC lines obtained after 3 weeks) defined a gene as significantly enriched in hESC if the average signal fold change (FC) between the hESC and the reference sample was larger than two and the gene in hESC sample was present. This analysis identified 1232 transcripts that were enriched in both H1 and hES-NCL1 compared with more differentiated progeny (Fig. 2C). Addition of another seven hESC lines (FES21, FES22, FES29, FES30, HS181, HS235 and HS237) to this comparison reduced the list of ESC-specific transcripts to 235 (representing 206 genes and ESTs; Fig. 2C, and for a complete list, see Supplementary Material, Table S1), thereby highlighting the validity of our hypothesis. Most importantly, the list of hESC-specific genes comprised several well-known hESC markers already identified in other studies such as *OCT4*, *NANOG*, *CD24*, *GDF3*, *TDGF1*, *TERF1*, *GABRB3*, *POLR3G*, *LECT1*, *DPPA4*, *GALANIN*, *DNMT3B* and *LIN28* (14–24,34). In addition to the hESC-enriched transcripts, we were also interested to identify highly expressed genes in all nine cell lines and any potential overlaps between the two populations. To select highly expressed transcripts in both cell lines, the Genespring feature called 'filter on expression level' was used by applying a minimum cut-off point of 110 to normalized data from the nine cell lines. A list of 117 transcripts representing 85 genes and ESTs (Supplementary Material, Table S2) was identified. From this analysis, we observed that the most abundant class of transcripts expressed in both cell lines were ribosomal proteins followed by transcription factors and nucleic acid binding proteins and protein processing and trafficking systems, which is perhaps indicative of a high rate of protein turnover in hESC. This is in accordance with other studies which have used SAGE and MPSS as a technique for identification of genes highly expressed in hESC lines (11,20). Comparison of the 85 highly expressed genes and ESTs with the 206 hESC-enriched genes and ESTs showed that only two genes were shared between them (*HDCMA18P* and *CACNA2D3*). Investigation of several databases including NetAffix, NCBI, Unigene, etc. revealed that *HDCMA18P* is likely to be involved in RNA binding and processing, whereas the *CACNA2D3* (calcium channel voltage-dependent alpha2/delta3) is likely to mediate the influx of calcium ions into the cell upon membrane polarization. Both of the genes are novel, therefore further detailed investigations are needed before any conclusion can be reached regarding their function in hESC.

Other key pluripotency factors such as *OCT4*, *REX1*, *NANOG*, *LIN28*, *CD24* and *TERT* are not represented among the highly expressed transcripts. This shows that highly expressed genes, although being part of the molecular signature for the hESC, will not necessarily be part of the functional machinery of hESC that can be exploited further for directing their differentiation.

Identification of most changed transcripts between the two cell lines

Because the hES-NCL1 line was derived from day 8 blastocysts, we were interested to determine whether it showed significant changes in gene expression from the H1 line which is derived from day 5 embryos. Using the Genespring software, we identified genes that were unique to H1, unique to hES-NCL1 or differentially expressed between the two cell lines. To identify the genes unique to each cell line, we followed the criteria that the gene had to be present in three out of the three replicates for the target cell line and absent in three out of the three replicates for the reference cell line. This identified 61 genes present in H1 (0.27% of all transcripts present) but completely absent in hES-NCL1 (Supplementary Material, Table S3) and 49 genes which were present only in hES-NCL1 (0.22% of all transcripts present; Supplementary Material, Table S3). The differential expression of six of the uniquely expressed candidates was confirmed by real-time PCR analysis (Fig. 3B). The most differentially expressed transcripts were of various natures: about one-third is as yet uncharacterized on a functional level and more than 10% are involved in DNA transcription (Supplementary Material, Table S3). The H1 and hES-NCL1 lines have different karyotype (i.e. H1 is male, NCL-1 is female; Fig. 1B), and this might contribute to their unique expression pattern. However, this does not seem to be a major factor, because only 3/61 genes that are unique to H1 are located on the Y chromosome (Fig. 3A). It is highly likely that these genes do not represent important regulators of pluripotency or differentiation because both cell lines are capable of differentiating into multiple cell lineages. It is interesting, however, that the nine genes we investigated by real-time RT–PCR not only show changes in expression between the two hESC lines, but also between each line and the embryonic carcinoma cell line (NTera2-SP.12) which was used as a positive control (Fig. 3B). Although the embryonic carcinoma cells show chromosomal abnormalities, they do retain the capacity to differentiate into several lineages and express most of the genes normally found in hESC lines albeit not necessarily at exactly the same level. This again suggests that variability in the expression of the candidate genes we have selected through the microarray analysis is unlikely to affect the pluripotency or differentiation capacity of these cells; however, genes which differentially expressed between the two cell lines might be useful as a 'fingerprint' for each cell line.

Using the Genespring software, we also investigated genes that consistently show more than 2-fold expression changes between the two cell lines in three replica experiments. A stringent *P*-value was chosen to ensure significant differences between the two cell lines. Surprisingly, we found that only six genes which comprise 0.03% of the transcripts present in the two cell lines (Fig. 3A) fell into this category. The differential expression of three of these candidates (*SLC1A6*, *PDCD6* and *MNS1*) was also confirmed by real-time RT–PCR (Fig. 3B). These results are very similar to a study published by Carpenter *et al*. (21), which showed that only three genes out of 2802 cDNA clones showed differential expression between four hESC lines (H1, H7, H9 and H14). The number of the unique genes that we found for each hESC line together with the genes that are differentially expressed between them is significantly lower than what has been previously reported for other hESC lines such as HSF-1, HSF-6 and H9 (14) or HS181, HS235, HS237, FES21, FES22, FES29 and FES30 (23). These differences could be attributed to changes in number of replicates used in the gene expression studies [two replicates were used by Skottman *et al*. (23)], the number of hESC lines being compared or the stringency of gene selection criteria [present and marginal genes were used by Abeyta *et al*. (14)]. Our own unpublished data suggested that both the increase in number of replicates and selection of only genes deemed to be present reduced significantly the number of genes considered unique or differentially expressed for each cell line (for example, comparison of the two cell lines using the criteria of present or marginal in one out of three samples for each hESC line increased the number of genes that showed two or more FC to 64).

In summary, the percentage of genes that are differentially expressed between the hES-NCL1 cell line derived from day 8 embryos to H1 derived from day 5 embryos is only 0.52%. This is within the variability limits described for ESC derived from days 5–6 embryos such as HSF-1, HSF-6 and H9 (2.4–4.5%) (14) and HS181, HS235, HS237, FES21, FES22, FES29 and FES30 (2.1–3.6%) (23). Large-scale gene expression studies in lymphoblastoid cells lines derived from unrelated individuals have shown that up to 5% of the genes can vary from one individual to another (27). In view of this, we would like to suggest that changes in the gene expression between the two cell lines we have analysed are likely to be due to the changes in the genetic profile of the embryo rather than the developmental stage of the blastocyst from where they were derived. To verify this further, one will have to compare directly gene expression patterns between ICMs dissected from different stages of the blastocyst's development and hESC lines derived from earlier embryos such as morulae. This work is currently progressing within our group.

Identification of new hESC markers

One of our aims in this investigation was to identify new hESC markers; therefore, we collected RNA samples from days 6, 10, 14 and 21 EBs from the hES-NCL1 line and hybridized these samples to the human U133 Plus 2.0 array. Using the Genespring software and a stringent selection criterion of at least 4-fold downregulation between the hES-NCL1 line and each group of EBs collected at different days (days 6, 10, 14 and 21, respectively), four groups of transcripts were selected (Fig. 4A). A Venn diagram was drawn to identify the set of transcripts that were common to

A

Affymetrix no	Gene name	Genbank no	Description	Fold change hES-NCL1 vs H1	p value of fold change
1569110_x_at	*PDCD6*	BC020552	programmed cell death 6	-25.841	0.000035
235244_at	*LOC131076*	BF001285	hypothetical LOC131076	-9.91	0.000031
205174_s_at	*QPCT*	NM_012413	glutaminyl-peptide cyclotransferase (glutaminyl cyclase)	3.3	0.999948
203607_at	*INPP5F*	NM_014937	inositol polyphosphate-5-phosphatase	3.5	0.99956
1554593_s_at	*SLC1A6*	BC028721	solute carrier family 1 (high affinity aspartate/glutamate transporter), member 6	3.06	0.99954
219703_at	*MNS1*	NM_018365	meiosis-specific nuclear structural protein 1	6.5	0.999727

B

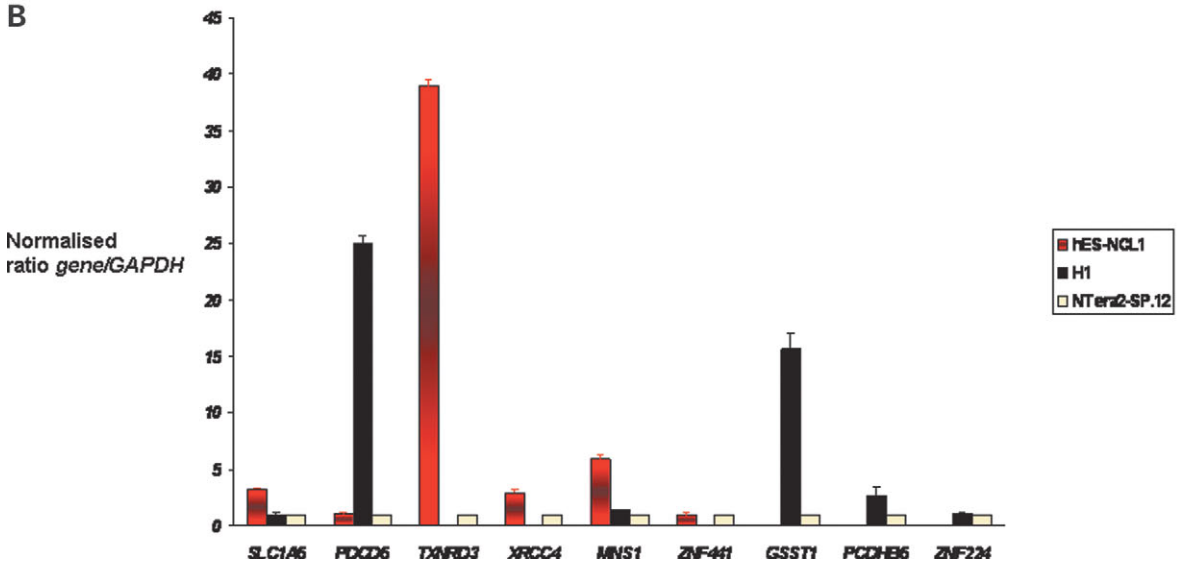

Figure 3. Identification of most changed transcripts between the two cell lines. (**A**) Genes that show more than 2-fold change in expression between H1 and hES-NCL1 cell lines. Change in *P*-value is calculated using the Wilcoxon's signed-rank test and ranges from 0.0 to 1.0 and provides a measure of the likelihood of change and direction. *P*-values close to 0.0 indicate likelihood for an increase in transcript expression level in the experiment array (H1) compared with the baseline (hES-NCL1), whereas *P*-values close to 1.0 indicate likelihood for a decrease in transcript expression in the experiment array (H1) compared with the baseline (hES-NCL1). (**B**) Real-time RT–PCR analysis for three genes that show differential expression between the two cell lines (*MNS1*, *SLC1A6*, *PDCD6*), three genes that are unique to H1 (*GSTT1, PCDHB6, ZNF224*) and three genes that are unique to hES-NCL1 (*TXNRD3*, *XRCC4*, *ZNF441*). A sample of embryonic carcinoma cells (NTera2-SP.12) was used as a positive control and normalized to 1 in each real time RT–PCR experiment. All other values were calculated with respect to this.

all the four subsets and indicated genes that were expressed in the hES-NCL1 but were downregulated 4-fold or more at all differentiation time points examined. One hundred and eighteen transcripts which represented 105 genes were identified and among those the major category comprised uncharacterized transcripts and genes involved in signalling pathways (Fig. 4B, and for a complete list, see Supplementary Material, Table S4).

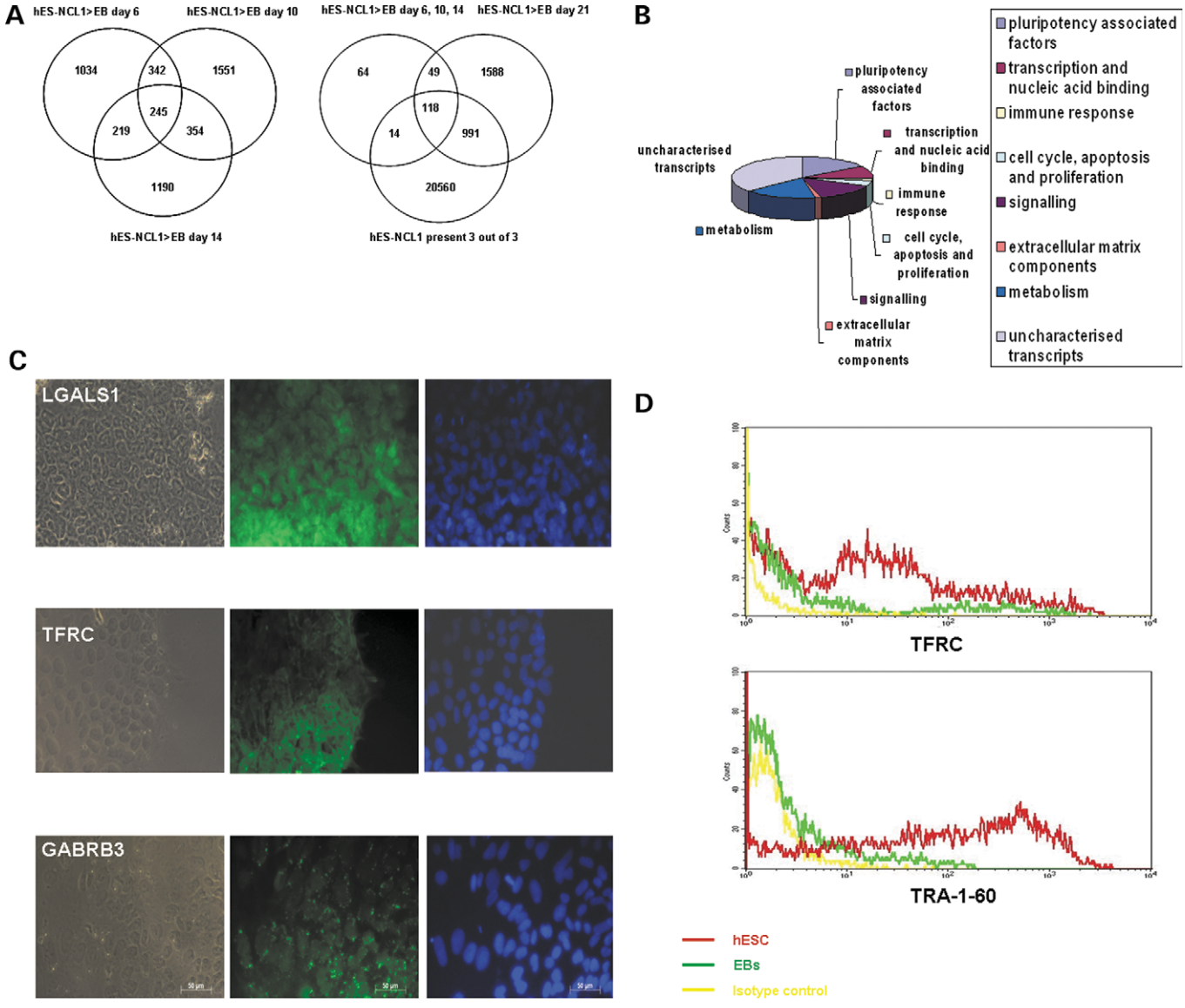

Figure 4. Identification of new hESC markers. (**A**) Identification of transcripts that are enriched in hESC and downregulated at least 4-fold compared with EBs collected at days 6, 10, 14 and 21. The Venn diagram on the left shows the selection of 245 common transcripts between the three groups selected previously on the basis of at least 4-fold downregulation from hES-NCL1 to EBs at days 6, 10 and 14, respectively. The Venn diagram on the right shows the cross comparison of these 245 transcripts (Venn diagram on the left) to genes present in all three replicates of hES-NCL1 and the group of transcripts that show at least 4-fold downregulation from hES-NCL1 to day 21 EBs. (**B**) Pie chart analysis showing the functional characterization of 105 genes that are enriched in hESC compared with EBs. (**C**) Immunocytochemistry for LGALS1, TFRC and GABRB3 in hES-NCL1 (similar images were obtained in the H1 cell line, data not shown). Immunofluorescence images for each antibody are shown in the middle panels. Bright field images are shown on the left panels and cell nuclei by DAPI staining are shown in the right panels. (**D**) Flow cytometry analysis for the expression of TFRC and TRA1-60 in hES-NCL1 and day 14 EBs (the same results were obtained using the H1 cell line, data not shown).

It is interesting to note that 12.38% of the identified transcripts have been already associated with maintenance of pluripotency in human and mouse ESC previously (*OCT4*, *NANOG*, *TDGF1*, *GDF3*; Supplementary Material, Table S4) or selected on the basis of higher expression in ESC versus EBs (*GAL*, *SEMA6A*, *LECT1*, *FLJ10884*, *POLR3G*, *LGALS1*, *GABRB3*, *TFRC*, *TERF1*, *DPPA4*, *DNMT3B*, *NODAL*, *HESX*, *PRDM14*) by other groups (14–23). Preliminary studies in murine and human ESC have already revealed a role for *DNMT3B*, *NODAL*, *POLR3G* and *GAL* in cell growth, viability and maintenance of pluripotency (28–35). In view of the published evidence and availability of commercial antibodies for some of these factors, we decided to investigate in further detail the expression and localization of LGALS1, TFRC and GABRB3 in hESC (Fig. 4C). LGALS1 also known as galectin1 can restrict carcinoma cell growth via suppression of RAS/MEK/ERK signalling pathway and induction of p21 and p27 transcription (36). This evidence seems to suggest that the high and selective expression of LGALS1 in hESC is required for maintaining ESC homeostasis and perhaps preventing a tumorigeneic expansion; however, further work is

needed to verify this suggestion. The transferrin receptor, TFRC, acts normally as a gatekeeper for maintaining iron homeostasis by mediating endocytosis of its ligand, iron-loaded transferrin, and high expression of this receptor has been observed in human mesenchymal stem cells and mESC (37,38). However, ablation of this gene in murine embryos suggests that transferrin and its receptor TFRC are mostly required for development of haematopoietic cells such as erythrocytes and lymphocytes but they are not essential for development of other tissues (38,39). The human GABA A receptor subunit beta 3 (GABRB3) was found to be an imprinted gene and a possible candidate for Prader–Willi syndrome (40), and the downregulation of its paternal allele in murine embryos results in a neurodevelopmental disorder which mimics Angelman syndrome (41); however, no functional role in stem cells has been described so far. A recent paper described the successful use of γ-aminobutyric acid and pipecolic acid which enhances GABA A receptor responses together with FGF2, $LiCl_2$ and TGFβ in defined medium to grow and derive new hESC lines (42). This was based on previous reports which indicated that GABA can stimulate proliferation of both neural and non-neural tissue (43) and microarray results similar to the ones presented here (15). Expression differences for these three genes were examined by flow cytometry (both intra and extracellular, data not shown) and immunocytochemistry (Fig. 4C). This indicated that TFRC is the only marker with cell surface expression; therefore, we compared TFRC expression with that of TRA-1-60 in hESC and day 14 EBs by flow (Fig. 4D). This analysis showed that 4% of the cells maintained the expression of TFRC after 14 days of differentiation; however, this was also the case with TRA-1-60 staining, suggesting that TFRC may serve as a new marker to distinguish hESC from cells present in EBs.

Signalling pathways in hESC

The second largest category of transcripts enriched in hESC similar comprised the genes involved in signalling pathways (Figs 4B and 5A). Interestingly, a significant number of those candidates fell within three major signalling categories belonging to the RAS/MAPK/ERK signalling pathway (*G3BP*, *RASAL2*, *SOS1* and *ITGB1BIP3*), the PI3K/AKT (*PI3KCB* and *PTEN*) and NFκβ signalling (*LCK*, *PELLINO1* and *TNSF11*).

The RAS/MAPK/ERK, PI3K/AKT and NFκβ signalling pathways identified above represent novel pathways that have not been thoroughly investigated in hESC. These pathways are very complex and involve a large number of components, and to facilitate the unfamiliar reader, we have outlined them schematically in Figure 5B.

RAS is a small GTPase responsible for transducing signals from a vast array of receptor tyrosine kinases and other receptors. RAS itself is regulated by GTPase-activating proteins (GAPs), which alternate signalling. RAS GAP transduces signals downstream of RAS in a MAPK-dependent manner (Fig. 5B, top panel). RAF serine/threonine protein kinases are considered to be the primary RAS effectors and are normally localized in the cytosol in inactive form. However, c-RAF (also known as RAF1) associates with RAS at the plasma membrane after growth factor-induced RAS guanine nucleotide exchange and its activation, which links a series of phosphorylation and changes in subcellular localization, links RAS to mitogen and extracellular-regulated kinase (MEK1/2) and MAPK. RAF directly phosphorylates and activates the protein kinase MEK1/2 which in turn phosphorylates and activates MAPK/ERK1 and MAPK/ERK2 (Fig. 5B, top panel). Activated MAPK/ERKs are then translocated from the cytoplasm to the nucleus where they activate nuclear transcription factors leading to changes in gene expression (Fig. 5B, top panel). *Pi3K* enzymes are normally regulated by growth factors and serve to phosphorylate phospholipids at the plasma membrane (Fig. 5B, bottom panel). Activated PI3K phosphorylates PIP_2 and generates PIP_3 which acts as a second messenger. AKT interacts with PIP_3 and subsequently translocates to the plasma membrane. *AKT* also referred as PKB plays a critical role in controlling the balance between survival and apoptosis (Fig. 5B, bottom panel) and is activated by phospholipid binding and activation loop phosphorylation at threonine 308 by PDK1 and phosphorylation at the C-terminus at serine 473. It is inactivated by PTEN phosphatase. AKT promotes cell survival by inhibiting apoptosis through its ability to phosphorylate and inactivate several target genes such as BAD, c-RAF and caspase-9 (Fig. 5B, bottom panel). In addition, it regulates glycogen synthesis through phosphorylation and inactivation of GSK3β and GSK3α. Activation of AKT survival signalling pathways leads to phosphorylation of Iκβ, the cytoplasmic inhibitor of nuclear factor κβ (NFκβ). Phosphorylation of Iκβ initiates proteasome-dependent degradation and allows NFκβ to enter the nucleus and regulate NFκβ-dependent gene expression (Fig. 5B, bottom panel).

Ras-GTPase-activating protein, SH3-domain-binding protein (G3BP1), was downregulated more than 4-fold during the differentiation of hESC (Fig. 5A). G3BP1 binds to the SH3 domain of Ras GAP and is shown to act as a Ras effector in breast cancer cell lines (44). Complete ablation of this gene in mouse results in embryonic lethality indicating an important role during embryonic development (45). Other activators of the pathway, such as RASAL2 and SOS1, which are guanine nucleotide exchange factors are also downregulated at the transcriptional level during differentiation, implying a greater role for RAS/MAPK signalling in hESC (Fig. 5A). We observed that one of the integrin β1 binding proteins, *ITGB1BP3*, which has been shown to affect laminin deposition and myogenic differentiation (46,47) is expressed at much higher levels in ESC compared with EBs (Fig. 5A). We investigated other members of the RAS/MAPK/ERK signalling pathway (Supplementary Material, Table S5) and noticed that several other components (*MAP4K1*, *MAP2K6*, *MAP3K7*, *MAP4K3*, *RAF1*, *MAPK13*, *MAPK9*, *MAPK6*, *MAPK1*/*ERK1*, *MAP2K1*, *KRAS*, *MAP3K4*, *NRAS*, *BRAF*) were transcriptionally downregulated during the differentiation process, albeit less than 4-fold. Taken together these insights acquired from the transcriptional study suggest a role for the RAS/MAPK/ERK signalling pathway in hESC.

Our transcriptional data also suggested a downregulation of several components of the NFκβ signalling pathway such as

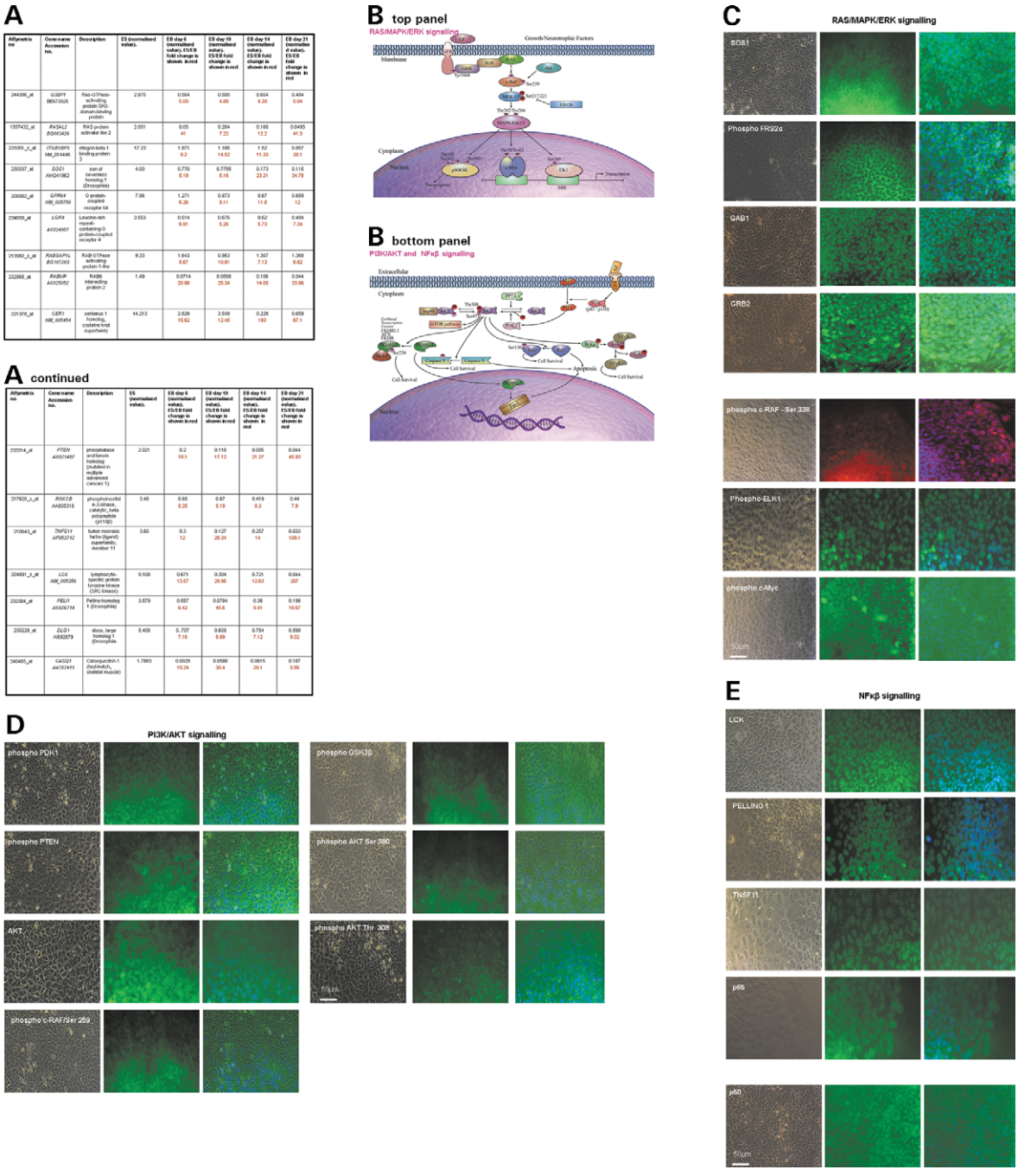

Figure 5. Expression of main components involved in signalling pathways in hESC. (**A**) Expression of transcripts involved in signalling pathway that are enriched in hESC compared with EBs. (**B**) Schematic presentation of three signalling pathways: RAS/MAPK/ERK (top panel), PI3K/AKT kinase and NFκβ (bottom panel). (**C**) Immunocytochemistry for components of RAS/MAPK signalling pathways in hESC. Immunofluorescence images for each antibody are shown in the middle panels. Bright field images are shown on the left panels and the overlap of cell nuclei by DAPI staining (in blue) and antibody staining (in green) is shown in the right panels. (**D**) Immunocytochemistry for components of PI3K/AKT signalling pathways in hESC. Immunofluorescence images for each antibody are shown in the middle panels. Bright field images are shown on the left panels and the overlap of cell nuclei by DAPI staining (in blue) and antibody staining (in green) is shown in the right panels. (**E**) Immunocytochemistry for components of NFκβ signalling pathways in hESC. Immunofluorescence images for each antibody are shown in the middle panels. Bright field images are shown on the left panels and the overlap of cell nuclei by DAPI staining (in blue) and antibody staining (in green) is shown in the right panels. (**F**) Top panel: flow cytometry analysis for various components of RAS/MAPK/ERK signalling pathway in hESC (hES-NCL1 line) and day 14 EBs (identical results were obtained with H1 line, therefore this data is not shown). Bottom panel: western blot analysis of several components of MAPK/ERK signalling pathways in hESC (H1 line) and day 14 EBs; GAPDH is used as a loading control. (**G**) Flow cytometry analysis for various components of PI3K/AKT signalling pathway in hESC (hES-NCL1 line) and day14 EBs (identical results were obtained with H1, therefore this data is not shown). (**H**) Flow cytometry analysis for various components of NFκβ signalling pathway in hESC (hES-NCL1 line) and day14 EBs (identical results were obtained with H1, therefore this data is not shown). (**I**) Hybridization of hESC (labelled with Cy3) and day 14 EB extracts (labelled with Cy5) to Panorama antibody cell signalling assays for various components of RAS/MAPK/ERK, PI3K/AKT and NFκβ signalling pathways. A ratio >1.0 indicates higher expression in hESC than EBs and ratio <1.0 indicates higher expression in EBs compared with hESC.

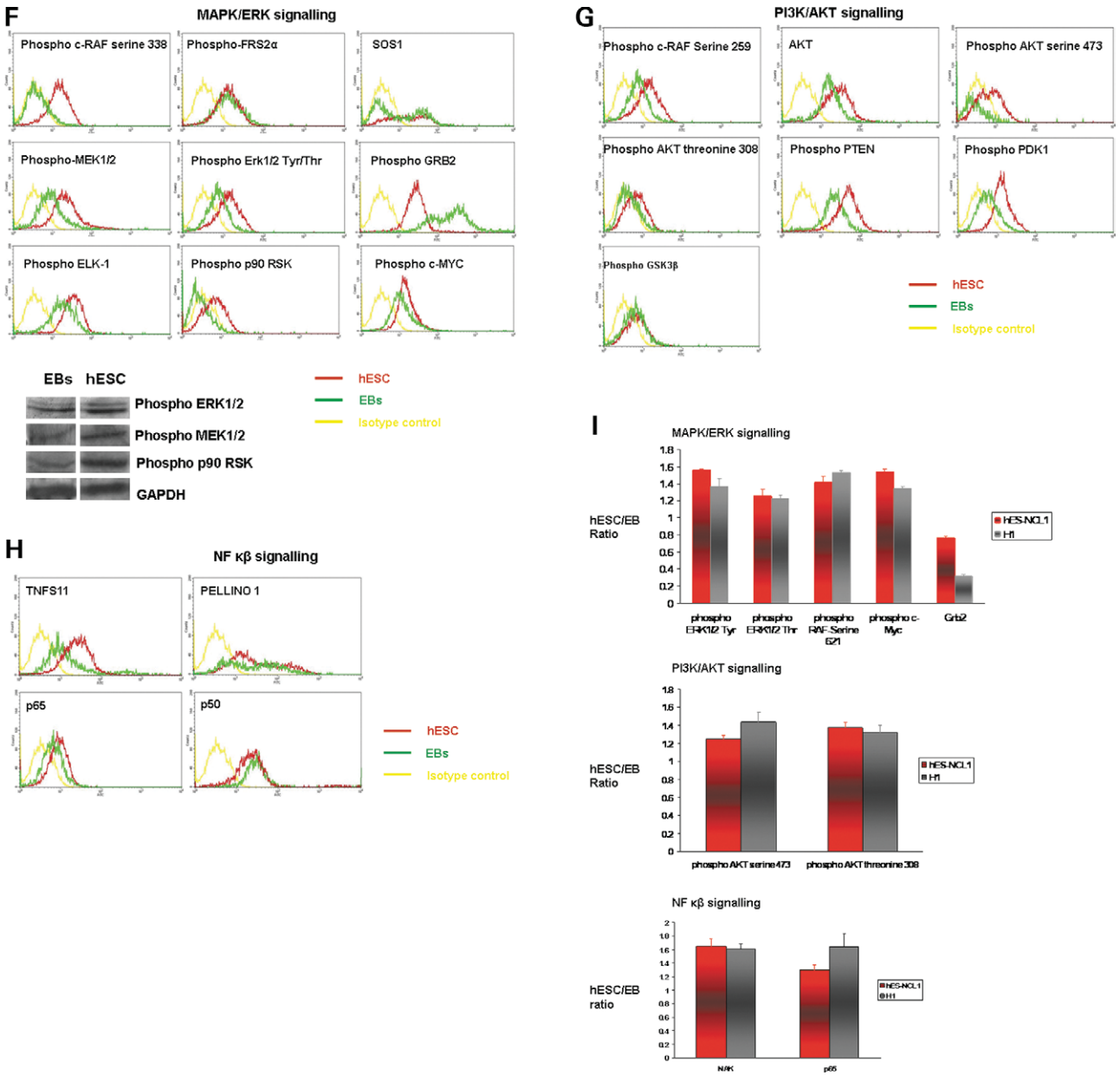

Figure 5. *Continued.*

LCK, *PELLINO1* and *TNFS11/ RANKL* (Fig. 5A). LCK, a lymphocyte-specific tyrosine kinase, (Src kinase) required for the activation of the NFκβ signalling pathway (47) has been shown to be downregulated during mESC differentiation (48). In addition, the product of another candidate gene, *PELLINO1*, identified in this screen is required for NFκβ activation, probably through interactions with IRAK and tumour necrosis factor receptor associated factor TRAF6 (49). Other members of these signalling pathways were either absent (TLRs) or slightly upregulated (Supplementary Material, Table S5). However, as for most of the signalling pathways, phosphorylation/translocation of key components as well as abundance of ligands/activators plays the most important role. In view of these, we looked carefully at NAK (NFκβ activating enzyme; Supplementary Material, Table S5) which showed less than 4-fold downregulation during the differentiation process and the IKBKε (which enhances the stability of Iκκs and therefore downregulates NFκβ activity) which was absent in both hESC lines and upregulated during the differentiation process (Supplementary Material, Table S5). Most importantly, the receptor activator of nuclear factor (NFκβ) ligand (RANKL/TNFS11) which is also enriched in hESC compared with EBs has been shown to be translationally regulated by PDK1 via the PI3K/AKT pathway suggesting a potential link between these two pathways (50,51). Interestingly, PDK1 activates NFκβ signalling by phosphorylating IKKβ which leads to its degradation and therefore allowing NFκβ p65 to enter the nucleus (51,52).

AKT has also been shown to be involved in transactivation of p65 and subsequent NFκβ-dependent transcription (52). These data seem to suggest an intrinsic link between the NFκβ and PI3K/AKT signalling pathways in other cell lines; however, this has not been explored previously in hESC. Of interest is the finding that PI3K/AKT pathway has been shown to be important for the maintenance of pluripotency in mESC (53), whereas FGF2 which is necessary for hESC growth activates ERK signalling (54–56). In view of this, it is important to investigate whether FGF2 signalling activates PI3K/AKT pathway in addition to MAPK/ERK signalling in hESC.

Although our transcriptional data suggest that the three selected pathways, PI3K/AKT, NFκβ and MAPK signalling, might be important for proliferation and maintenance of pluripotency in hESC, in-depth studies to investigate the role of these pathways in hESC and potential links between them have not been carried out as yet. We investigated the expression of some crucial components of these three pathways in hESC and changes during their differentiation to EBs. Immunocytochemistry on both H1 and hES-NCL1 on various components of these three signalling pathways (see Fig. 5C, D and E for RAS/MAPK, PI3K/AKT and NFκβ signalling pathways, respectively) demonstrated cytoplasmic/cell membrane localization for the phosphorylated form FRS2α and nuclear localization for phospho-ELK1 and c-MYC (Fig. 5C). The phosphorylated form of c-RAF serine 338 as well as GAB1, SOS1 and GRB2 showed both nuclear and cytoplasmic/cell membrane localization (Fig. 5C). Most of the components of the PI3K/AKT pathway (phospho-GSK3β, phospho-c-RAF serine 259, phospho-PDK1 and phospho-AKT threonine 308) showed cytoplasmic/cell membrane localization and a few (unphosphorylated AKT, phospho-AKT serine 308 and phospho-PTEN) displayed both nuclear and cytoplasmic/cell membrane localization (Fig. 5D). In contrast, all the tested components of the NFκβ pathway showed nuclear localization with the exception of TNSF11 which showed some additional spotty expression in the cytoplasm (Fig. 5E). We were unable to detect the expression of phospho-MEK1/2, phospho-ERK1/2 (also known as p44/42) and phospho-90 RSK (Fig. 5B) which suggests that they might be expressed at lower levels. To improve the detection sensitivity and assess changes between hESC and EBs, we carried out flow cytometry analysis for all the components involved in these pathways for which commercial antibodies were available (Fig. 5F–H). This showed that the key components of the RAS/MAPK/ERK pathway (phospho-c-RAF serine 338, phospho-MEK1/2, phospho-ERK1/2, phospho-ELK1, phospho-c-MYC and phospho-p90; Fig. 5F), PI3K/AKT pathway (phospho-PDK1, phospho-PTEN, phospho-AKT serine 473 and phospho-AKT threonine 308, phospho-c-RAF serine 259; Fig. 5G) and NFκβ pathway (phospho-65 and TNFS11; Fig. 5H) were all downregulated during differentiation. For some of the MAPK/ERK signalling pathway, this downregulation was confirmed by western blotting (Fig. 5F, lower panel). To confirm our initial flow cytometry results, we also took advantage of the panorama Ab microarray for cell signalling components where a good percentage of the antibodies of interest are spotted in duplicate on nitrocellulose filters. We hybridized hESC and day 14 EB cell extract to those arrays and calculated the ratio of hESC/EB for each protein of interest (Fig. 5I). This analysis confirmed our flow cytometry results and suggested that hESC expressed higher levels of key components of the MAPK/ERK signalling pathways (phospho-ERK1/2, phospho-c-RAF and phospho-c-MYC) as well as the PI3K/AKT (phospho-AKT serine 473 and phospho-AKT threonine 308) and NFκβ pathways (p65 and NAK- NFκβ-activating kinase). These results were confirmed by dye reversal experiment (Supplementary Material, Fig. S1). In both experiments, we observed that hESC/EB ratio for GRB2 was different in each of the cell lines. Investigation of the normalized values for GRB2 in the two cell lines showed very similar expression (Supplementary Material, Table S5); however, different expression was observed in day 14 EBs obtained from the two different hESC lines. This transcriptional difference could account for rather different hESC/EB ratios in the two cell lines.

FGF, BMP/TGFβ and WNT signalling have been implicated in the maintenance of pluripotency in human ESC (54–56). In view of these, we investigated our microarray data for the expression of main components of these signalling pathways. A close investigation of the FGF2 signalling pathway indicated an abrupt downregulation of FGF2 during the differentiation process as well as two of the FGF target genes, *c-FOS* and *c-KIT* (Supplementary Material, Table S5). This is in accordance with other published findings which demonstrate a crucial role for FGF2 in maintaining the pluripotency of hESC (54–56). Investigation of the BMP/TGFβ signalling pathways suggested that a large number of the components of this pathway were present in undifferentiated hESC, although some time at minimal levels (Supplementary Material, Table S5). Like other researchers, we found that *NODAL* and two of its inhibitors *LEFTY1* and *LEFTY2* were expressed in human ESC, but they were abruptly downregulated upon differentiation suggesting a tight control of this signalling pathway in pluripotency hESC (16,54). Interestingly, ALK5 that has been implicated in the TGFβ signalling is the only one among the ALKs that show downregulation upon differentiation, thus providing further support for the role of TGFβ in maintaining the hESC pluripotency as suggested by Amit *et al*. (3). Most interestingly, two inhibitors of Activin A and BMP signalling, *FOLLISTATIN* and *BAMBI* (BMP and Activin membrane bound inhibitor) are greatly increased upon differentiation, whereas a third inhibitor, CERBERUS, shows an abrupt decrease upon differentiation. Vallier *et al*. (54) suggested that Activin/Nodal pathway in co-operation with FGF2 is necessary for the maintenance of pluripotency in hESC. Our data does corroborate these findings. In spite of this, it highlights once more the complexity of these pathways and the fine tune imposed not only by ligands and receptors, but also by specific inhibitors.

MAPK/ERK, PI3/AKT and NFκβ are important for maintenance of pluripotency and viability in human ESC

To validate the importance of these signalling pathways for maintenance of pluripotency and viability of hESC, we used three inhibitors: Ly294002 (10 μM) which is a specific PI3 kinase inhibitor already shown to interfere with the

maintenance of pluripotency in mESC (57), U0126 (20 and 30 μM) a specific MEK1/2 inhibitor and sodium pyrrolidinethiocarbamate (PTDC) (50 μM) a specific NFκβ inhibitor which prevents p65 entry into the nucleus. Inhibitors concentration was chosen carefully based on the criteria of inhibiting the chosen pathway without causing other non specific effects. In the case of U0126, lower concentrations (10 μM) did not result in inhibition of MAPK/ERK even after 5–30 min of application. This could be due to the presence of FGF2 in the medium which activates ERK signalling and counteracts the effects of U0126; therefore, higher concentrations of this inhibitor (20–60 μM) were tested, 50 and 60 μM caused extensive cell death. Therefore, we selected the lowest concentrations (20 and 30 μM) at which inhibition of the MAPK/ERK signalling pathway was evident. The same logic was applied for the NFκβ inhibitor, although published literature recommends a much higher effective concentration (100 μM) compared with the other two inhibitors. We noticed that at 50 μM concentration, the entry of p65 into the nucleus was inhibited (Fig. 6H) and the effects on cell differentiation and death were the same as when 100 μM PTDC was applied; therefore, 50 μM PTDC was used in all the following experiments.

Two to three days after the application of PTDC and LY294002, cell differentiation was prominent in the middle of hESC colonies compared with the control which was vehicle alone (Fig. 6A). Cell differentiation was not evident in the lower (20 μM) U0126 concentration (Fig. 6A); however, this was observed as soon as the U0126 concentration was increased to 30 μM (data not shown). In addition, significant cell death was present when cells were treated with U0126 and PTDC as assessed by Annexin V staining (Fig. 6B). The increase in U0126 concentration also caused an increase in total cell death which reached 62.6% at 30 μM. The amount of differentiation was assessed by alkaline phosphatise staining (Fig. 6C), real-time RT–PCR analysis for *OCT4*, *NANOG* and *SOX2* (Fig. 6D) and flow cytometry for SSEA-4 (Fig. 6E). In the case of LY294002 and PTDC, a significant reductions in *OCT4*, *NANOG* and *SOX2* expression and AP staining and the percentage of SSEA-4-positive cells (Fig. 6C–E) were observed, suggesting loss of pluripotency upon inactivation of PI3K/AKT and NFκβ signalling pathways. This was also evident at the higher concentration of U0126 (30 μM; Supplementary Material, Fig. S2A and B) but not at the 20 μM concentration (Fig. 6B–E).

PI3K inactivation by LY294002 resulted as expected in downregulation of the phosphorylated AKT kinase (both serine 473 and threonine 308) and the downstream targets of AKT kinase such as phosphorylated form of GSK3β and c-RAF (serine 338; Fig. 6F and I). In addition, it resulted in downregulation of several components of the MAPK/ERK pathway such as the phosphorylated form of MEK1/2, ERK1/2 and one of the intracellular effectors, phosphorylated form of c-MYC (Fig. 6F and I). The active form of AKT has been shown to directly phosphorylate and activate c-RAF (58) (Fig. 5B), and from our results, it is obvious that inhibition of the PI3/KAKT pathway results in downregulation of the phosphorylated form of c-RAF (serine 338). Because the active form of c-RAF phosphorylates MEK1/2, we are inclined to speculate that the observed downregulation of the other components of the MAPK/ERK signalling pathway does not simply reflect the process of differentiation ongoing in these cells but rather reflects a direct link between the PI3K/AKT and MAPK/ERK pathway occurring at the level of c-RAF (Fig. 7). Application of LY294002 also resulted in reduction of phosphorylated form of p65; however, inhibition of the NFκβ pathway did not result in inactivation of the PI3K/AKT pathway (Figs 6F, H, I and 7) suggesting that the PI3K/AKT pathway acts upstream of the NFκβ pathway. It is widely reported in the literature that activated AKT kinase phosphorylates Ikκs, which serve as cytoplasmic sequestrators of p65 and p50. Phosphorylation of Ikκs results in their ubiquitination and subsequent degradation (Fig. 5B) and translocation of the activated p65/p50 complex into the nucleus. Our initial results suggest that this is also likely to be the case for hESC; however, further investigation into the Ikκs and their expression and function in hESC is required.

In several tumour cell lines, p65 expression has been observed in both cytoplasm and nucleus, and activation of the NFκβ pathway is marked by translocation of the cytoplasmic form of p65 into the nucleus where together with p50 it activates transcription of several genes. Immunocytochemistry in both hESC cell lines indicated that p65 and p50 are observed only in the nucleus (Fig. 5E). Application of PTDC, a known inhibitor of the NFκβ pathway, inhibits the translocation of p65 to the nucleus and this is evident following addition of PTDC to hESC cultures where several nuclei without p65 expression are duly observed (Fig. 6H). As expected, no changes in p50 expression or localization were observed. Downregulation of nuclear p65 expression caused loss of viability as well as differentiation of hESC highlighting the importance of NFκβ pathway in the maintenance of viability and pluripotency (Fig. 6A–E).

Inhibition of the MAPK/ERK signalling pathway by U0126 resulted as expected in decrease in the phosphorylated form of ERK1/2 and one of its downstream effectors, the phosphorylated form of p90, RSK (Fig. 6G). It is worth mentioning that no changes were observed in the expression of most of the components of the PI3K/AKT pathway (phospho-AKT serine 473 and threonine 308, phospho-PDK1, phospho-GSK3β and phospho-c-RAF), whereas inhibition of PI3K/AKT pathway resulted in downregulation of most of the components of MAPK/ERK signalling cascade (Fig. 6F). These results imply that MAPK/ERK signalling is downstream of the PI3K/AKT kinase. Inhibition of the MAPK/ERK signalling at the level of MEK1/2 does not seem to affect two of the components of the NFκβ pathway (Fig. 6G); however, inhibition of the NFκβ pathway results in downregulation of the activated form of ERK1/2 and its downstream effector, p90 RSK (Fig. 6H and I), implying that NFκβ pathway acts upstream of the MAPK/ERK signalling pathway. These results are summarized in a table (Fig. 6I) and schematically outlined in Figure 7.

DISCUSSION

Elucidation of the signalling events that govern the self-renewal and pluripotency of hESC is important for understanding their physiology and devising optimal culture

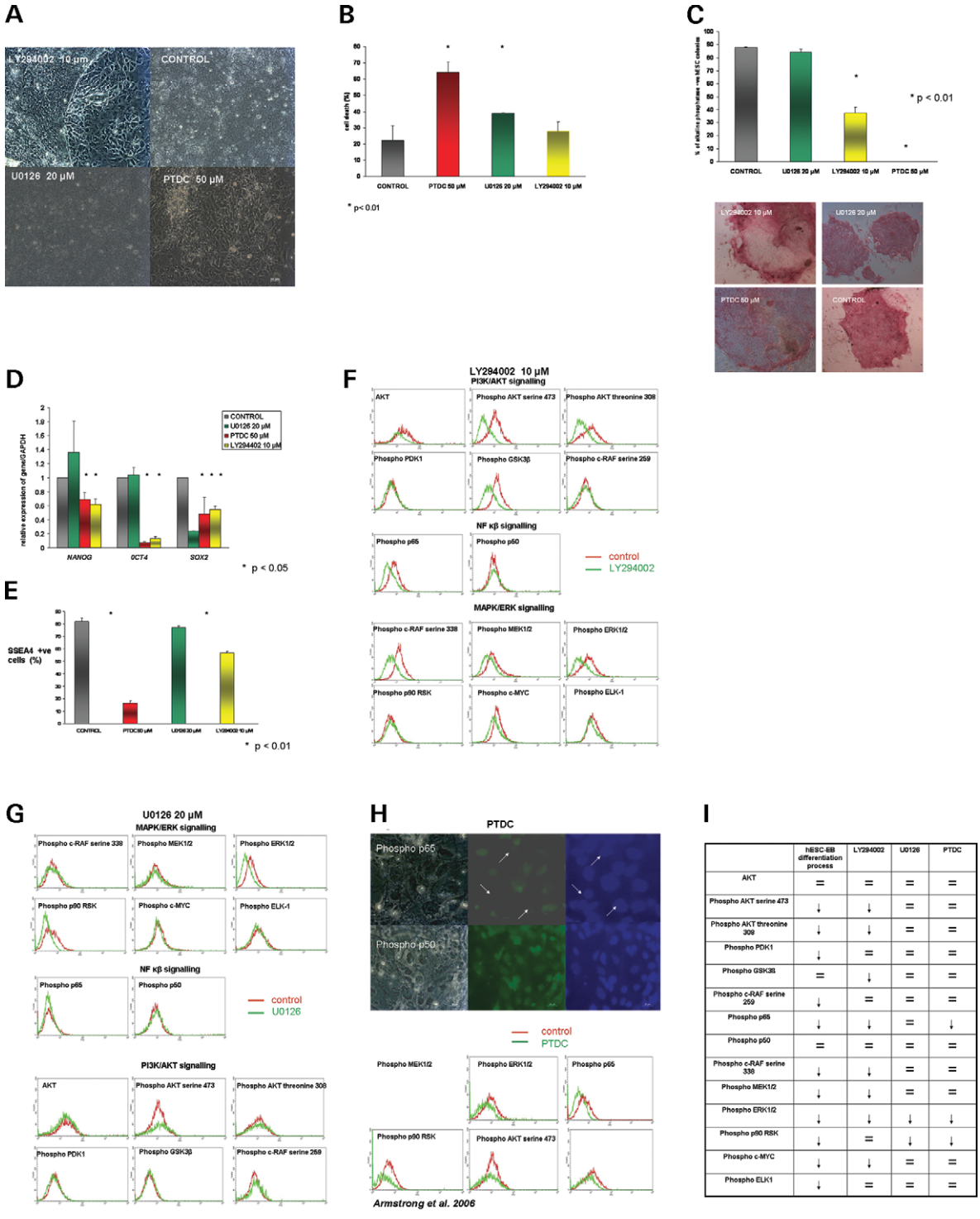

Figure 6. MAPK/ERK, PI3K/AKT and NFκβ signalling is important for the maintenance of pluripotency and viability in hESC (hES-NCL1 is shown; however, similar results were obtained with H1). (**A**) Photographs of hESC 4 days after the application of three inhibitors. (**B**) Viability of hESC after the application of LY294002, U0126 and PTDC. (**C**) hESC pluripotency after application of LY294002, U0126 and PTDC measured by AP staining. (**D**) hESC pluripotency after application of LY294002, U0126 and PTDC assessed by real-time RT–PCR for the expression of *NANOG*, *OCT4* and *SOX2*. (**E**) Flow cytometry analysis for the expression of SSEA4 after application of LY294002, U0126 and PTDC. (**F**) Flow cytometry analysis of the main components of PI3K/AKT kinase, MAPK/ERK and NFκβ signalling after the application of LY294002. (**G**) Flow cytometry analysis of the main components of PI3K/AKT kinase, MAPK/ERK and NFκβ signalling after the application of U0126. (**H**) Top panel: immunocytochemistry analysis for the expression of phospho-p65 and p50 in hESC after the application of PTDC. Bright field images are shown in the left panels, antibody staining in the middle panels and cell nuclei staining by DAPI in the right-hand panels. The white arrows indicate nuclei that have lost p65 expression. Bottom panel: flow cytometry analysis of the main components of PI3K/AKT kinase, MAPK/ERK and NFκβ signalling after the application of PTDC. (**I**) Summary of changes in expression of the main components of PI3K/AKT kinase, MAPK/ERK and NFκβ signalling pathways during differentiation of hESC to EBs and after the application of LY294002, PTDC and U0126.

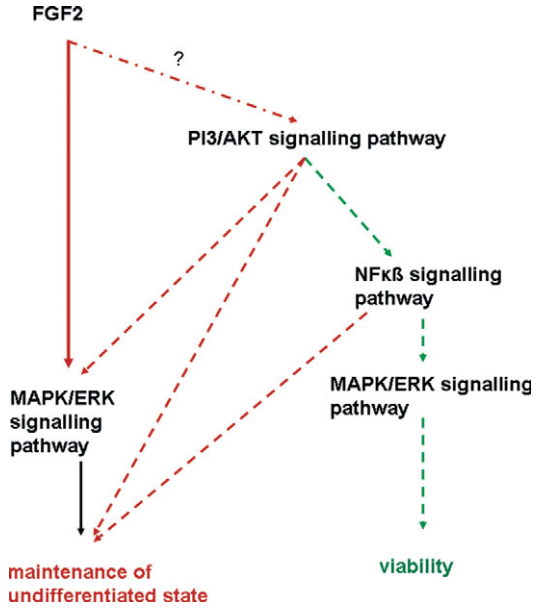

Figure 7. Schematic presentation of likely signalling events in hESC. FGF2 has been shown to maintain hESC pluripotency by activating MAPK/ERK signalling pathways (this is indicated by uninterrupted lines). Our own data suggest that MAPK/ERK and NFκβ act downstream of the PI3K/AKT pathway and these three pathways are important for maintenance of the undifferentiated state and viability (this is indicated by interrupted lines). A possible link between FGF2 and subsequent activation of PI3K/AKT pathway that is not proven as yet is indicated by a question mark.

conditions for their large-scale growth. It is of equal importance to understand the changes which take place in such signalling networks as a cause or consequence of hESC differentiation, as this may help us to devise better strategies to direct differentiation into particular developmental pathways. This will be of paramount importance to our efforts to produce defined populations of cells for therapeutic use. Transcription factors such as *OCT4* (59) and *NANOG* (60) are indispensable for the maintenance of pluripotency in hESC but it has recently become evident that activation of FGF2 signalling (61) or ERK activation (55) and its co-operation with the Activin/Nodal signalling pathway (54) are necessary to maintain the pluripotency of hESC. Substantial differences exist in a number of key signalling pathways between human and mouse ESC; for example, LIF/Stat3 and Bmp4 signalling which are important for maintenance of pluripotency in mESC do not play the same role in hESC (12,13,61,62). In striking contrast to mESC which display high ERK1/2 activity when they are stimulated to undergo differentiation, hESC display high basal activity of ERK1/2 in the undifferentiated state which correlates with large amounts of endogenous, high molecular mass FGF2 (63). These fundamental differences highlight the need for new and thorough signalling studies in hESC *per se*.

We undertook a large transcriptional study which was focused on the molecular characterization of a new cell line derived by our group from a day 8 blastocyst (hES-NCL1) and highlighted important changes in gene expression during differentiation to EBs. We identified an interesting phenomenon in that the second largest group of transcripts downregulated during differentiation of hESC were components of several important signalling pathways, namely PI3K/AKT, RAS/MAPK/ERK and NFκβ signalling. Using a combination of flow cytometry, western blotting and an antibody signalling array, we confirmed that the majority of factors involved in these signalling pathways and identified by our large-scale transcriptional study were downregulated during the differentiation of hESC, indicating a possible role in the maintenance of pluripotency and viability in hESC. This hypothesis was further confirmed by using specific inhibitors for each of the signalling pathways (LY294002 for PI3K/AKT, U0126 for MAPK/ERK and PTDC for NFκβ) which caused loss of pluripotency and viability at specific concentrations. These results are not entirely surprising given the contribution of the aforementioned signalling pathways in a number of human cancers (64) and during embryogenesis (65–67).

A number of studies conducted in mouse embryos have shown that most of the MAPK/ERK pathway proteins were present in trophoblast and the inner cell mass at embryonic day 3.5, where they may mediate mitogenic signals within the embryo or coming from the uterus (65). Most importantly, knockouts of FRS2α, Gab1, Grb2, Sos-1, Raf-B and Raf1 result in peri-implantation or placental lethality (66) and this could well be due to defects in formation of placental trophoblasts given the role of Ras in extraembryonic endoderm differentiation (67). In this context, it worth mentioning two main differences between the human and the murine system that can help with further interpretation of our results. First, in mouse, FGF/MAPK signalling seems to be involved in trophoblast and thus placental development (68,69), whereas in the humans, relatively high and stable concentration of FGF2 is needed to maintain the proliferation and pluripotency of hESC (61). Secondly, in the murine system, the suppression of MAPK/ERK signalling by BMP4 promotes the self-renewal of mESC and aids their derivation (70–72), whereas in the human, addition of BMP4 causes differentiation of hESC to trophoectoderm (13). This suggests a different role for MAPK/ERK signalling in hESC and our results show that this is indeed the case. We observed significant cell death in hESC cultures treated with 20 μM of MEK1/2 inhibitor (U0126) and this increased with increasing concentrations of inhibitor. No prominent loss of hESC morphology and pluripotency was observed at the 20 μM concentration of U1026, whereas an increase in U0126 concentration to 30 μM caused cell differentiation as described in our Results and Supplementary Material, Figure S2. While this manuscript was under preparation, two reports described the dosage-dependent effect of FGF2 on hESC renewal (61) and ERK activation by FGF2 in hESC (55) and this perhaps explains the dosage-dependent effects of U0126. Interestingly, in the murine system, the orthologue of the human *ERAS* gene plays an important role in the proliferation of mESC; however, this gene does not bind to Raf or activate the MAPK cascade (73). This together with our data would suggest that other RAS family components such as K-RAS and H-RAS, also enriched in hESC compared to EBs (56) (Supplementary Material, Table S5), or other downstream components of the MAPK cascade activate MAPK/ERK in hESC more than in the differentiated cells of the EBs. Although these biochemical assays remain to be carried out in hESC, our results strongly suggest an efficient

downregulation of several important components of the MAPK/ERK cascade during hESC differentiation at both transcriptional and translational/post-translational level and a crucial role for the MAPK/ERK activation in hESC.

Extensive work in mESC has suggested that the PI3K pathway plays an important role in proliferation, tumourigenicity and maintenance of the undifferentiated state (reviewed in 74). We found that most of the active components of the PI3K/AKT pathway such as the phosphorylated form of AKT and PDK1 are downregulated during hESC differentiation to EBs and inactivation of this pathway results in differentiation. In addition, we observed a downregulation in the active components of the MAPK/ERK and NFκβ pathways, whereas inactivation of these in isolation did not disrupt those of the PI3K/AKT pathway suggesting that MAPK/ERK and NFκβ act downstream of the PI3K/AKT kinase. This is not completely unexpected or surprising. Current literature suggests that in other human cell types, AKT and PDK1 phosphorylate Ikκs (52,53), which serve as cytoplasmic sequestrators of p65 and p50. Phosphorylation of Ikκs results in their ubiquitination and subsequent degradation and translocation of the activated p65/p50 complex into the nucleus which initiates NFκβ-dependent transcription; therefore, high activity of PI3K/AKT would be reflected in a more active NFκβ signalling. Our results support a role for PI3K/AKT-dependent activation of the NFκβ signalling cascade in maintenance of viability and the undifferentiated state in hESC. Activation of the MAPK/ERK pathway by PI3K/AKT has also been documented in several other stem cells (murine haematopoietic stem cells (75) and germ cells (*Xenopus* oocytes) (76), and although the mechanisms involved are not fully understood, our data and others point to PI3K/AKT-dependent MAPK/ERK activation at some point between RAS and MEK1/2. However, further work is needed to verify this hypothesis.

It is interesting that FGF2 has been suggested to act via activation of the MAPK/ERK pathway (55,63). Our results highlight that MAPK/ERK and NFκβ signalling are likely to act downstream of the PI3K/AKT pathway and that the majority of the active components of the three signalling pathways are downregulated during hESC differentiation to EBs which takes place in the absence of FGF2. This raises an intriguing possibility that FGF2 initiates a hierarchical signalling cascade (outlined in Fig. 7) with sequential activation of PI3K/AKT, MAPK/ERK and NFκβ cascades. If this is the case, monolayer differentiation in the absence of FGF2 should result in similar downregulation of the active components of these pathways and our own preliminary data indicate that this is indeed the case (Armstrong and Lako, unpublished data). Our inhibitor study was conducted in the presence of FGF2; however, if the above hypothesis is true, one would expect more dramatic effects if inhibition of these signalling pathways was carried out in the absence of FGF2. This work is currently in progress within our group.

Our results suggest that activation of the MAPK/ERK is important for the maintenance of viability in hESC and this is dependent on the activation of the NFκβ cascade, already shown to govern cell survival and play a similar role in many human cancer cell types (77,78). This raises intriguing questions as to whether the mechanisms involved in maintenance of the undifferentiated state and viability in hESC are similar to the ones observed in cancer cells. This may help to understand some of the mechanisms involved in karyotypic abnormalities observed in 'culture-adapted hESC', which result in clonal selection and escape from FGF2-dependent signalling (79,80).

A detailed molecular and functional characterization of all the cell lines derived by different labs at various stages of embryonic development, in view of the differences in their ability to differentiate *in vitro* to different lineages observed by us and others, is essential for our understanding of hESC biology (14,18,22,23). Our transcriptional study of a well-characterized cell line derived from day 8 embryos, hES-NCL1 (25), has shown that the developmental stage from which the cell line is derived does not enhance the molecular differences between different cell lines that are more likely to result from their different genetic profile. We have used these data to isolate new cell surface markers such as transferrin receptor (TFRC) that can be used to separate hESC from differentiated cells. We were unable to identify any other novel cell surface markers specific for hESC; however, we are currently performing bioinformatic analysis on the uncharacterized and novel transcripts which comprised 33.6% of the genes we identified to be enriched in hES-NCL1.

Our study for the first time has used flow cytometry analysis to characterize a large number of components involved in three signalling pathways. The validity of the method is supported by other techniques such as western blotting and antibody arrays. Using these techniques, we have added new intracellular markers which can be used to compare hESCs with differentiated progeny. This knowledge can now be used to aid definition of GMP-compatible media for large-scale growth of hESC. Examples of this approach already exist; for example, γ-aminobutyric acid and pipecolic acid have been used in defined hESC medium to derive new stem cell lines based on enhanced expression of GABA A receptor subunit beta 3 (42) in hESC. Interestingly, we have shown in this manuscript that the transferrin receptor is enriched in hESC compared with EBs. Not surprisingly, transferrin is used in other hESC defined media (54). On a similar note, small molecules that activate PI3K/AKT, MAPK/ERK and NFκβ cascades can be investigated for this purpose. Similarly, small molecules that inhibit the specific pathways can also be explored for setting off specific differentiation pathways in hESC.

Understanding how the specification events occur in the human pre-implantation embryos has been difficult to dissect in humans given the lack of sufficient embryonic material. On this basis, we feel that our functional investigation of signalling pathways in hESC will shed some light on the biological events during pre-implantation development and will help with new methods to derive embryonic stem cell lines suitable for clinical purposes.

MATERIALS AND METHODS

Culture and differentiation of hESC

Human ESC were grown on mitotically inactivated mouse embryonic fibroblasts with hESC medium containing

Knockout-DMEM (Invitrogen, Paisley, UK), 100 μM β-mercaptoethanol (Sigma, Dorset, UK), 1 mM L-glutamine (Invitrogen), 100 mM non-essential amino acids (Invitrogen), 20% serum replacement (SR, Invitrogen), 1% penicillin–streptomycin (Sigma) and 8 ng/ml FGF2 (Invitrogen). hESC medium was changed daily. hESC were passaged by incubation in 1 mg/ml collagenase IV (Invitrogen) for 5–8 min at 37°C or mechanically dissociated and then removed to freshly prepared feeders. EB differentiation was induced by harvesting hESC with collagenase as described above and culturing them in suspension in Knockout DMEM medium (Invitrogen) containing 20% fetal calf serum (FCS) (Hyclone), 1 mM L-glutamine (Invitrogen), 100 mM non-essential amino acids (Invitrogen), 100 μM β-mercaptoethanol (Sigma) and 1% penicillin–streptomycin (Sigma).

Karyotype analysis of hESC

The karyotype of hESC was determined by standard G-banding procedure.

Flow cytometry analysis of hESC

For the flow cytometry analysis, the hESC were collected using collagenase IV treatment (1 mg/ml for 5 min) followed by brief accutase incubation (Chemicon). hESC were suspended in staining buffer [phosphate-buffered saline (PBS) +5% FCS] at concentration of 10^6 cells/ml. About 10^5 cells were stained with TRA1-60, TRA1-81, SSEA-3, SSEA-4 (10 μg/ml final concentration, Chemicon), CD117 and CD135 (10 μg/ml final concentration, BD Biosciences, Oxford, UK). Several washes were carried out in staining buffer before proceeding to staining with secondary antibodies (goat anti-mouse IgG/M conjugated to FITC). Intracellular staining was performed by fixing the cells for 10 min in 0.5% formaldehyde followed by gentle permeabilization in ice-cold 90% methanol. The permeabilized cells were washed three times in staining buffer before being stained with the primary antibodies for 30 min at room temperature. The primary antibodies were purchased from Cell Signaling Technologies as part of the phospho-Akt pathway sampler kit (phospho-AKT-serine 473, phospho-AKT-threonine 308, AKT, phospho-GSK3β-serine 9, phospho-c-RAF-serine 259, phospho-PTEN-serine 380 and phospho-PDK1-serine 241) or phospho-ERK1/2 pathway sampler kit (phospho-c-RAF serine 338, phospho-MEK1/2 serine 217/221, phospho-ERK1/2-threonine 202/tyrosine 204, phospho-p90 RSK-serine 380, phospho-ELK-1 serine 383) or as separate unconjugated antibodies (phospho-c-MYC threonine 58/serine 62, phospho-p65 serine 536). The other antibodies were purchased from R&D systems (TFRC, PTEN), Abcam (GABA A receptor beta3, GPR64, phospho-NFκβ p50 serine 529), Santa Cruz Biotechnology Inc. (GALECTIN-1, phospho-FRS2/tyrosine 436, GRB2/C-23, Sos1/H-122, GAB1/H-198 and phospho-c-RAF serine 338) and Chemicon (LCK, TNFS11/RANKL). All antibodies were used at concentrations suggested by the manufacturers unless otherwise stated. Three washes in staining buffer were carried out before staining with secondary antibody, goat anti-mouse IgM/G-FITC (6 μg/ml final concentration; Sigma) or donkey anti-rabbit IgM/G-FITC (6 μg/ml final concentration; Sigma). Cells were washed again three times and resuspended in staining buffer before being analysed with FACS Calibur (BD) using the CellQuest software. Ten thousand events were acquired for each sample and propidium iodide staining (1 μg/ml) was used to distinguish live from dead cells for extracellular markers.

Immunostaining and fluorescence microscopy

Cells were fixed with 4% paraformaldehyde for 10 min and permeabilized with 0.1% Triton X-100 and 5% FCS in PBS at room temperature for 45 min. The cells were incubated at room temperature for 17 h with the primary antibodies described earlier (1:100 dilution) and subsequently washed with 5% FCS and PBS before addition of the appropriate secondary antibody (Rhodamine-conjugated anti-goat IgG from Jackson ImmunoResearch, 1:100, was used to detect phospho-c-RAF serine 338 purchased from Santa Cruz, whereas for the rest FITC-conjugated anti-rabbit immunoglobulins from Sigma-Aldrich, 1:100, were applied). The cells were washed before fluorescence microscopy and the images were collected using a Zeiss microscope and Axiovert software.

Western blotting

Cell lysates were electrophoresed on a 10% SDS–PAGE gel and electrophoretically transferred to a polyvinylidene difluoride membrane (Hybond-P, Amersham). Membranes were blocked in Tris-buffered saline with 5% milk and 0.1% Tween. The blots were probed with phospho-ERK1/2 kinase (Cell Signaling Technology, 1:1000), phospho-p90 RSK (Cell Signaling Technology, 1:1000), phospho-MEK1/2 (Cell Signaling Technology, 1:1000), GAPDH (Abcam, 1:2000) overnight and revealed with horseradish peroxidase-conjugated secondary anti-rabbit antibody (Amersham Biosciences, 1:20 000). Antibody/antigen complexes were detected using ECL reagent (Amersham Biosciences) and GeneSnap software (version 4.00.00, SYNGENE) with GeneGnome (SYNGENE). Bands were analysed using the GeneTools software (version 3.00.22, SYNGENE).

Inhibitor studies

MEK1/2 inhibitor (U0126), PI3K inhibitor (LY2940002) and NFκβ inhibitor (PTDC) were purchased from Sigma. The hESC were plated in matrigel in the presence of MEF conditioned medium as described in Stojkovic *et al*. (25). Inhibitors were added the following day and medium was changed every day for the following 6 days of culture. The choice of inhibitors concentration (10 μM for LY2940002, 20 and 30 μM for U0126 and 50 μM for PTDC) was based on other published reports for mESC and our empirical trials.

Cell signalling assays

Panorama Ab microarray for cell signalling containing 224 different antibodies spotted in duplicate on nitrocellulose-

coated glass were purchased from Sigma. One milligram of hESC (H1 and hES-NCL1) and EB cell extracts was collected, labelled with Cy3 and Cy5, respectively, and hybridized to the slides according to manufacturer's instructions. Dye reversal experiments were also carried out for the hES-NCL1. Cy3 and Cy5 signals were read on Gene Pix Pro 4.0 and normalization in each case was carried out using as reference the beta-actin house keeping protein included in the chip. The hESC/EB ratio was calculated using MS Excel. A ratio >1.0 indicates higher expression in hESC than EBs and ratio <1.0 indicates higher expression in EBs compared with hESC.

Microarray analysis

Total RNA was extracted from hESC and EBs at days 6, 10, 14 and 21 using Trizol (Invitrogen), and 10 μg of the RNA sample was used to make biotin-labelled cRNA (copy RNA) according to manufacturer's instructions. Following appropriate clean-up of the cRNA (IVT cRNA clean-up spin column as supplied with Affymetrix gene chips), biotin-labelled cRNA was quantified and fragmented by metal-induced hydrolysis according to manufacturer's protocol (Affymetrix, Buckinghamshire, UK). This converts full-length cRNA into fragments of 35–200 bp in length which are suitable for hybridization. Prior to hybridization, a test array of housekeeping controls was analysed to determine sample suitability for GeneChip arrays. Biotin-labelled cRNAs produced in this manner were hybridized to the Human U133 Plus 2 array and washed according to manufacturer's protocol. The MAS 5.0 software detection algorithm (Affymetrix) was used to determine the presence (P), absence (A) or marginal expression (M) of each gene in the array. The data obtained from MAS 5.0 were then normalized and further analysed in the GeneSpring software 6.2 (Silicon Genetics). Per chip normalization was done as follows. Values below 0.01 were set to 0.01 and then each measurement was divided by the 50th percentile of all measurement in that sample. A gene was nominated as differentially expressed between the two cell lines if change call was increased or decreased and the change P-value was <0.05. A gene was defined as significantly upregulated if the signal fold change (FC) between the target and reference sample was larger than 2 and the target sample was present. Alternatively, a gene was defined as significantly downregulated if the FC was less than -2 and the reference sample was present. As suggested by the manufacturer, the probe sets were excluded if the detection call for both the target and the reference were 'absent' or if no change call (NC) was detected (NC, change $P > 0.05$). Only the genes that fulfilled all the filtering criteria reproducibly in three biological replicates were considered significant. In testing for the reproducibility of the samples (H1 and hES-NCL1), correlation coefficients of the normalized signal intensities of the replicate samples were calculated. These calculations were performed automatically in MS Excel using Pearson's correlation coefficient formula (given subsequently). The signal intensity values from the samples were pasted into an MS Excel spreadsheet. The statistical function CORREL was chosen from the functions wizard, the values from the samples to be compared were selected and finally the correlation coefficient of the two samples being compared was presented.

$$r = \frac{\Sigma XY - (\Sigma X \Sigma Y / N)}{\sqrt{(\Sigma X^2 - (\Sigma X)^2/N)(\Sigma Y^2 - (\Sigma Y)^2/N)}}$$

Where X is the normalized signal intensities from H1, Y the normalized signal intensities from hES-NCL1 and N the number of normalized signal intensities in each sample.

RT–PCR analysis

RT was carried out using the cells of cDNA II kit (Ambion, Huntingdon, UK) according to manufacturer's instructions. In brief, hESC were submerged in 100 μl of ice-cold cell lysis buffer and lysed by incubation at 75°C for 10 min. Genomic DNA was degraded by incubation with DNAse I for 15 min at 37°C. RNA was reverse transcribed using M-MLV reverse transcriptase and random hexamers following manufacturer's instructions. PCR reactions were carried out using the following primers:

*OCT4*F: 5′-GAAGCTGGAGAAGGAGAAGCTG-3′;
*OCT4*R: 5′-CAAGGGCCGCAGCTTACACATGTTC-3′;
*REX1*F: 5′-GCGTACGCAAATTAAAGTCCAGA-3′;
*REX1*R: 5′-CAGCATCCTAAACAGCTCGCAGAAT-3′;
*NANOG*F: 5′-GATCGGGCCCGCCACCATGAGTGTGGATCCAGCTTG-3′;
*NANOG*R: 5′-GATCGAGCTCCATCTTCACACGTCTTCAGGTTG-3′;
*TERT*F: 5′-CGGAAGAGTGTCTGGAGCAAGT-3′;
*TERT*R: 5′-GAACAGTGCCTTCACCCTCGA-3′;
*GAPDH*F: 5′-GTCAGTGGTGGACCTGACCT-3′;
*GAPDH*R: 5′-CACCACCCTGTTGCTGTAGC-3′.

PCR products were run on 2% agarose gels and stained with Ethidium bromide. Results were assessed on the presence or absence of the appropriate size PCR products. Reverse transcriptase negative controls were included to monitor genomic contamination.

LightCycler real-time PCR analysis

Real-time PCR analysis was carried out using QuantiTect SYBR Green PCR Master mix (Qiagen). The reaction was performed with 1 μl cDNA per 20 μl reaction and each reaction was performed in triplicate. The LightCycler experimental run protocol used was: PCR activation step (95°C for 15 min), amplification with data acquisition repeated 50 times (94°C for 15 s, annealing temperature for primers for 30 s, 72°C for 20 s with a single fluorescence data collection), melting curve (60–95°C with a temperature transition rate of 0.1°C/s and continuous fluorescence data collection) and finally cooling to 40°C. The crossing point (CP) for each transcript was determined using second derivative maximum method in the LightCycler software v3.5.3 (Roche Diagnostics). *GAPDH* CP for each sample was used as the internal control of these real-time analyses. The data were analysed using the LightCycler relative quantification software v1.01 (Roche Diagnostics). For each gene, the value for the hESC

was set to 1 (100%) and all other values were calculated with respect to this. Statistical significance of the results was assessed using Student's *t*-test ($P < 0.05$). PCR reactions were carried out using the following primers:

*GDF3*F: 5′-GTCCGCGGGAATGTACTTCG-3′;
*GDF3*R: 5′-CACCTTGTGGCCATGGGACT-3′;
*NANOG*F: 5′-AGAAGGCCTCAGCACCTAC-3′;
*NANOG*R: 5′-GGCCTGATTGTTCCAGGATT-3′;
*OCT4*F: 5′-TCTCGCCCCCTCCAGGT-3′;
*OCT4*R: 5′-GCCCCACTCCAACCTGG-3′;
*SOX2*F: 5′-GGCAGCTACAGCATGATGCAGGAGC-3′;
*SOX2*R: 5′-CTGGTCATGGAGTTGTACTGCAGG-3′;
*AFP*F: 5′-TGCAGCCAAAGTGAAGAGGGAA-3′;
*AFP*R: 5′-ATAGCGAGCAGCCCAAAGAAGA-3′;
*KDR*F: 5′-CAGACGGACAGTGGTATGGT-3′;
*KDR*R: 5′-AGCCCAGATTCTCCAGCCTG-3′;
*PDCD6*F: 5′-CGGACCAGAGCTTCCTGTGG-3′;
*PDCD6*R: 5′-ACACACCCGTGAACTCGCTG-3′;
*ZNF224*F: 5′-TCGTAGCCATCACGGAGCTG-3′;
*ZNF224*R: 5′-ACCCAGGGCATCAGCTTCTG-3′;
*GAPDH*F: 5′-GTCAGTGGTGGACCTGACCT-3′;
*GAPDH*R: 5′-CACCACCCTGTTGCTGTAGC-3′;
*SLC1A6*F: 5′-CTGCAGCATCACGGCCACAG-3′;
*SLC1A6*R: 5′-CCGTCCCCGGGATGCCCCCT-3′;
*TXNRD3*F: 5′-ACTTTGTTCTGGCCTCTTGA-3′;
*TXNRD3*R: 5′-GTGAATTCCAATGGTGTCAT-3′;
*XRCC4*F: 5′-TTCAAGTCTTGATGTCACTG-3′;
*XRCC4*R: 5′-TTCTAAAGACATGTTTTCAG-3′;
*MNS1*F: 5′-CAGTTGCAGCAAAGGCGGCA-3′;
*MNS1*R: 5′-GTAATCCCAGCTACTCAGGA-3′;
*ZNF441*F: 5′-AAGGCTGGGTATGGTGGCTC-3′;
*ZNF441*R: 5′-GTAAAGGGTCCTCCACATTG-3′;
*GSST1*F: 5′-GTCCTCACATCTCCTTAGCT-3′;
*GSST1*R: 5′-CATGGGCCTCCTGGAAGAGG-3′;
*PCDHB6*F: 5′-GGTCGCTACTCGGTGCCCGA-3′;
*PCDHB6*R: 5′-TCATATTGTCAAGTACCCTC-3′;
*PAX6*F: 5′-GAATCAGAGAAGACAGGCCA-3′;
*PAX6*R: 5′-CGCCTGGATATGCGCCAGCT-3′.

Population doubling time assays

Human ESC colonies were harvested by collagenase treatment and subjected to accutase digest for 2 min at room temperature. Live cells were counted using Trypan blue (Sigma) exclusion. Fifty thousand live cells were added to each well of a four-well plate containing mitotically inactivated mouse embryonic fibroblasts and 0.5 ml of human ESC medium with basic fibroblast growth factor. Cells were permitted to grow for 5 days and cell numbers were estimated using Trypan blue exclusion method. The number of population doublings was estimated as $\mathrm{PD} = \ln(n_2/n_1)/\ln 2$, where n_1 was the seeded cell amount and n_2 the obtained cell amount.

Apoptosis assay

Cells undergoing apoptosis can be enumerated using the Annexin V-FITC apoptosis detection kit (BD Biosciences-Pharmingen) in which FITC-conjugated Annexin V binds to the externalized phosphatidyl serine characteristic of apoptotic cells. The protocol was carried out in accordance with manufacturer's instructions and briefly comprises the following. Cells were harvested using accutase, washed twice with ice-cold PBS and counted. 1×10^5 cells are suspended in 100 μl of 1 × binding buffer (supplied), then 5 μl of Annexin V-FITC and 5 μl of propidium iodide solution are added. The mixture is vortexed gently and incubated for 15 min at room temperature in the dark. About 400 μl 1 × binding buffer is added and the cells are analysed by flow cytometry (FACS Caliber, Becton Dickinson).

AP staining

AP staining was carried out using the Alkaline Phosphatase Detection Kit following manufacturer's instructions (Chemicon, Temecula, CA, USA; www.chemicon.com). Briefly cells were fixed in 90% methanol and 10% formamide for 2 min and then washed with rinse buffer (20 mM Tris–HCl pH 7.4, 0.05% Tween-20) once. Staining solution (Naphthol/Fast Red Violet) was added to the wells, and plates were incubated in the dark for 15 min. The bright field images were obtained using a Zeiss microscope and AxioVision software (Carl Zeiss, Jena, Germany).

SUPPLEMENTARY MATERIAL

Supplementary Material is available at HMG Online.

ACKNOWLEDGEMENTS

The authors are grateful to Dr Nick Allenby for help with the reading of antibody arrays, Dr Stefan Pryzborski for providing the NTera2-SP.12 embryonic carcinoma cell line, Simon Foster for help with the diagrams and Dennis Kirk for technical assistance. In particular, we would like to thank Dr Heli Skottman for sharing the raw data from seven human ESC lines after hybridization to Affymetrix Chip U133A and U133B. This study was supported by MRC grant no. G0301182, BBSRC grant no. BBS/B/14779, One North East Regional Development Agency and Life Knowledge Park. Funding to pay the Open Access publication charges for this article was provided by MRC UK grant number G0301182.

Conflict of Interest statement. The authors declare no conflict of interests.

REFERENCES

1. Thomson, J.A., Itskovitz-Eldor, J., Shapiro, S.S., Waknitz, M.A., Swiergiel, J.J., Marshall, V.S. and Jones, J.M. (1998) Embryonic stem cell line from human blastocysts. *Science*, **282**, 1145–1147.
2. Chambers, I. and Smith, A. (2004) Self-renewal of teratocarcinoma and embryonic stem cells. *Oncogene*, **23**, 7150–7160.
3. Amit, M., Shariki, C. and Margulets, V. (2004) Feeder layer- and serum-free culture of human embryonic stem cells. *Biol. Reprod.*, **70**, 837–845.
4. Klimanskya, I., Chung, Y., Meisner, L., Johnson, J., West, M. and Lanza, R. (2005) Human embryonic stem cells derived without feeder cells. *Lancet*, **365**, 1636–1641.

5. Zwaka, T.P. and Thomson, J.A. (2003) Homologous recombination in human embryonic stem cells. *Nat. Biotechnol.*, **21**, 319–321.
6. Gropp, M., Itsykson, P., Singer, O., Ben-Hur, T., Reinhartz, E., Galun, E. and Reubinoff, B.E. (2003) Stable genetic modification of human embryonic stem cells by lentiviral vectors. *Mol. Ther.*, **7**, 281–287.
7. Schulz, T.C., Palmarini, G.M., Noggle, S.A., Weiler, D.A., Mitalipova, M.M. and Condie, B.G. (2003) Directed neuronal differentiation of human embryonic stem cells. *BMC Neurosci.*, **4**, 27–41.
8. Chadwick, K., Wang, L., Li, L., Menendez, P., Murdoch, B., Rouleau, A. and Bhatia, M. (2003) Cytokines and BMP-4 promote hematopoietic differentiation of human embryonic stem cells. *Blood*, **102**, 906–915.
9. Ginis, I., Luo, Y., Miura, T., Thies, S., Brandenberger, R., Gerecht-Nir, S., Amit, M., Hoke, A., Carpenter, M.K., Itskovitz-Eldor, J. and Rao, M.S. (2004) Differences between human and mouse embryonic stem cells. *Dev. Biol.*, **269**, 360–380.
10. Hyslop, L.A., Armstrong, L., Stojkovic, M. and Lako, M. (2005) Human ES biology: clinical implications. *Exp. Rev. Mol. Med.*, **19**, 1–21.
11. Wei, C.L., Miura, T., Robson, P., Lim, S.K., Xu, X.Q., Lee, M.Y., Gupta, S., Stanton, L., Luo, Y., Schmitt, J. *et al*. (2005) Transcriptome profiling of human and murine ESCs identifies divergent paths required to maintain the stem cell state. *Stem Cells*, **23**, 166–185.
12. Daheron, L., Opitz, S.L., Zaehres, H., Lensch, W.M., Andrews, P.W., Itskovitz-Eldor, J. and Daley, G.Q. (2004) LIF/STAT3 signaling fails to maintain self-renewal of human embryonic stem cells. *Stem Cells*, **22**, 770–778.
13. Xu, R.H., Chen, X., Li, D.S., Li, R., Addicks, G.C., Glennon, C., Zwaka, T.P. and Thomson, J.A. (2002) BMP4 initiates human embryonic stem cell differentiation to trophoblast. *Nat. Biotechnol.*, **20**, 1261–1264.
14. Abeyta, M.J., Clark, A.T., Rodriguez, R.T., Bodnar, M.S., Pera, R.A. and Firpo, M.T. (2004) Unique gene expression signatures of independently-derived human embryonic stem cell lines. *Hum. Mol. Genet.*, **13**, 601–608.
15. Sperger, J.M., Chen, X., Draper, J.S., Antosiewicz, J.E., Chon, C.H., Jones, S.B., Brooks, J.D., Andrews, P.W., Brown, P.O. and Thomson, J.A. (2003) Gene expression patterns in human embryonic stem cells and human pluripotent germ cell tumors. *Proc. Natl Acad. Sci. USA*, **100**, 13350–11355.
16. Sato, N., Sanjuan, I.M., Heke, M., Uchida, M., Naef, F. and Brivanlou, A.H. (2003) Molecular signature of human embryonic stem cells and its comparison with the mouse. *Dev. Biol.*, **260**, 404–413.
17. Zeng, X., Miura, T., Luo, Y., Bhattacharya, B., Condie, B., Chen, J., Ginis, I., Lyons, I., Mejido, J., Puri, R.K. *et al*. (2004) Properties of pluripotent human embryonic stem cells BG01 and BG02. *Stem Cells*, **22**, 292–312.
18. Bhattacharya, B., Miura, T., Brandenberger, R., Mejido, J., Luo, Y., Yang, A.X., Joshi, B.H., Ginis, I., Thies, R.S., Amit, M. *et al*. (2004) Gene expression in human embryonic stem cell lines: unique molecular signature. *Blood*, **103**, 2956–2964.
19. Rao, R.R. and Stice, S.L. (2004) Gene expression profiling of embryonic stem cells leads to greater understanding of pluripotency and early developmental events. *Biol. Reprod.*, **71**, 1772–1778.
20. Richards, M., Tan, S.P., Tan, J.H., Chan, W.K. and Bongso, A. (2004) The transcriptome profile of human embryonic stem cells as defined by SAGE. *Stem Cells*, **22**, 51–64.
21. Carpenter, M.K., Rosler, E.S., Fisk, G.J., Brandenberger, R., Ares, X., Miura, T., Lucero, M. and Rao, M.S. (2004) Properties of four human embryonic stem cell lines maintained in a feeder-free culture system. *Dev. Dyn.*, **229**, 243–258.
22. Skottman, H., Stromberg, A.M., Matilainen, E., Inzunza, J., Hovatta, O. and Lahesmaa, R. (2005) Unique gene expression signature by human embryonic stem cells cultured under serum free conditions correlates with their enhanced and prolonged growth in an undifferentiated stage. *Stem Cells*, August 11 [Epub ahead of print].
23. Skottman, H., Mikkola, M., Lundin, K., Olsson, C., Stromberg, A.M., Tuuri, T., Otonkoski, T., Hovatta, O. and Lahesmaa, R. (2005) Gene expression signatures of seven individual human embryonic stem cell lines. *Stem Cells*, **23**, 1343–1356.
24. Strelchenko, N., Verlinsky, O., Kukharenko, V. and Verlinsky, Y. (2004) Morula-derived human embryonic stem cells. *Reprod. Biomed. Online*, **9**, 623–629.
25. Stojkovic, M., Lako, M., Stojkovic, P., Stewart, R., Przyborski, S., Armstrong, L., Evans, J., Herbert, M., Hyslop, L., Ahmad, S. *et al*. (2004) Derivation of human embryonic stem cells from day-8 blastocysts recovered after three-step *in vitro* culture. *Stem Cells*, **22**, 790–797.
26. Suarez-Farinas, M., Noggle, S., Heke, M., Hemmati-Brivanlou, A. and Magnasco, M.O. (2005) Comparing independent microarray studies: the case of human embryonic stem cells. *BMC Genom.*, **6**, 99.
27. Cheung, V.G., Conlin, L.K., Weber, T.M., Arcaro, M., Jen, K.Y., Morley, M. and Spielman, R.S. (2003) Natural variation in human gene expression assessed in lymphoblastoid cells. *Nat. Genet.*, **33**, 422–425.
28. Parisi, S., D'Andrea, D., Lago, C.T., Adamson, E.D., Persico, M.G. and Minchiotti, G. (2003) Nodal-dependent Cripto signaling promotes cardiomyogenesis and redirects the neural fate of embryonic stem cells. *J. Cell Biol.*, **163**, 3–14.
29. Minchiotti, G. (2005) Nodal-dependant Cripto signaling in ES cells: from stem cells to tumor biology. *Oncogene*, **24**, 5668–5675.
30. Jackson, M., Krassowska, A., Gilbert, N., Chevassut, T., Forrester, L., Ansell, J. and Ramsahoye, B. (2004) Severe global DNA hypomethylation blocks differentiation and induces histone hyperacetylation in embryonic stem cells. *Mol. Cell. Biol.*, **24**, 8862–8871.
31. Chen, T., Ueda, Y., Dodge, J.E., Wang, Z. and Li, E. (2003) Establishment and maintenance of genomic methylation patterns in mouse embryonic stem cells by Dnmt3a and Dnmt3b. *Mol. Cell. Biol.*, **23**, 5594–5605.
32. Hattori, N., Abe, T., Hattori, N., Suzuki, M., Matsuyama, T., Yoshida, S., Li, E. and Shiota, K. (2004) Preference of DNA methyltransferases for CpG islands in mouse embryonic stem cells. *Genet. Res.*, **14**, 1733–1740.
33. Huntriss, J., Hinkins, M., Oliver, B., Harris, S.F., Beazley, J.C., Rutherford, A.J., Gosden, R.G., Lanzendorf, S.F. and Picton, H.M. (2004) Expression of mRNAs for DNA methyltransferases and methyl-CpG-binding proteins in the human female germline, preimplantation embryos and embryonic stem cells. *Mol. Reprod. Dev.*, **67**, 323–336.
34. Enver, T., Soneji, S., Joshi, C., Brown, J., Iborra, F., Orntoft, T., Thykjaer, T., Maltby, E., Smith, K., Dawud, R.A. *et al*. (2005) Cellular differentiation hierarchies in normal and culture adapted human embryonic stem cells. *Hum. Mol. Genet.*, **14**, 3129–3140.
35. Tarasov, K.V., Tarasova, Y.S., Crider, D.G., Anisimov, S.V., Wobus, A.M. and Boheler, K.R. (2002) Galanin and galanin receptors in embryonic stem cells: accidental or essential? *Neuropeptides*, **4**, 239–245.
36. Fischer, C., Sanchez-Ruderisch, H., Welzel, M., Wiedenmann, B., Sakai, T., Andre, S., Gabius, H.J., Khachigian, L., Detjen, K.M. and Rosewicz, S. (2005) Galectin-1 interacts with the alpha 5beta 1 fibronectin receptor to restrict carcinoma cell growth via induction of p21 and p27. *J. Biol. Chem.*, **280**, 37266–37277.
37. Bai, J.Z., Ding, W.M., Liu, Z.J., Yu, M.J., Tian, J.H., Wang, F., Du, J., Zhang, X.Y., Li, L.S. and Shen, L. (2004) Transferrin receptor expression of human mesenchymal stem cells and *in vitro* tracking by autoradiography after transplantation in spinal cord. *Beijing Da Xue Xue Bao*, **36**, 276–280.
38. Ned, R.M., Swat, W. and Andrews, N.C. (2003) Transferrin receptor 1 is differentially required in lymphocyte development. *Blood*, **102**, 3711–3718.
39. Macedo, M.F., de Sousa, M., Ned, R.M., Mascarenhas, C., Andrews, N.C. and Correia-Neves, M. (2004) Transferrin is required for early T-cell differentiation. *Immunology*, **112**, 543–549.
40. Meguro, M., Mitsuya, K., Sui, H., Shigenami, K., Kugoh, H., Nakao, M. and Oshimura, M. (1997) Evidence for uniparental, paternal expression of the human GABAA receptor subunit genes, using microcell-mediated chromosome transfer. *Hum. Mol. Genet.*, **6**, 2127–2133.
41. Liljelund, P., Handforth, A., Homanics, G.E. and Olsen, R.W. (2005) GABAA receptor beta3 subunit gene-deficient heterozygous mice show parent-of-origin and gender-related differences in beta3 subunit levels, EEG, and behavior. *Brain Res. Dev. Brain Res.*, **157**, 150–161.
42. Ludwig, T.E., Levenstein, M.E., Jones, J.M., Berggren, W.T., Mitchen, E.R., Frane, J.L., Crandall, L.J., Daigh, C.A., Conard, K.R., Piekarczyk, M.S. *et al*. (2006) Derivation of human embryronic stem cells in defined conditions. *Nat. Biotech.*, **24**, 185–187.
43. Watanabe, M., Maemura, K., Kanbara, K., Tamayama, T. and Hayasaki, H. (2002) GABA and GABA receptors in the central nervous system and other organs. *Int. Rev. Cytol.*, **213**, 1–47.
44. Barnes, C.J., Li, F., Mandal, M., Yang, Z., Sahin, A.A. and Kumar, R. (2005) Heregulin induces expression, ATPase activity, and nuclear localisation of G3BP, a Ras signaling component in human breast tumors. *Cancer Res.*, **62**, 1251–1255.

45. Zekri, L., Chebli, K., Tourriere, H., Nielsen, F.C., Hansen, T.V., Rami, A. and Tazi, J. (2005) Control of fetal growth and neonatal survival by the RAS-GAP associated endoribonuclease G3BP. *Mol. Cell. Biol.*, **25**, 8703–8716.
46. Li, J., Rao, H., Burkin, D., Kaufman, S.J. and Wu, C. (2003) The muscle integrin binding protein (MIBP) interacts with alpha7beta1 integrin and regulates cell adhesion and laminin matrix deposition. *Dev. Biol.*, **261**, 209–219.
47. Kang, J.L., Lee, H.W., Kim, H.J., Lee, H.S., Castranova, V., Lim, C.M. and Koh, Y. (2005) Inhibition of SRC tyrosine kinases suppresses activation of nuclear factor- κβ, and serine and tyrosine phosphorylation of Iκβ-α in lipopolysaccharide stimulated RAW 264.7 macrophages. *J. Toxicol. Environ. Health A*, **68**, 1643–1662.
48. Meyn, M.A., 3rd., Schreiner, S.J., Dumitrescu, T.P., Nau, G.J. and Smithgall, T.E. (2005) Src family kinase activity is required for murine embryonic stem cell growth and differentiation. *Mol. Pharmacol.*, **68**, 1320–1330.
49. Jiang, Z., Johnson, H.J., Nie, H., Qin, J., Bird, T.A. and Li, X. (2003) Pellino 1 is required for interleukin-1 (IL-1)- mediated signalling through its interactions with the IL-1 receptor associated kinase 4 (IRAK4)-IRAK-tumor necrosis factor receptor associated factor 6 (TRAF6) complex. *J. Biol. Chem.*, **278**, 10952–10956.
50. Tominaga, Y., Tamguney, T., Kolesnichenko, M., Bilanges, B. and Stokoe, D. (2005) Translational deregulation in PDK-1 − /− embryonic stem cells. *Mol. Cell. Biol.*, **25**, 8465–8475.
51. Tanaka, H., Fujita, N. and Tsuruo, T. (2005) 3-Phosphoinositide-dependent protein kinase-1-mediated IkappaB kinase beta (IkkB) phosphorylation activates NF-kappaB signaling. *J. Biol. Chem.*, **280**, 40965–40973.
52. Sizemore, N., Leung, S. and Stark, G.R. (1999) Activation of phosphatidylinositol 3-kinase in response to interleukin-1 leads to phosphorylation and activation of the NF-kappaB p65/RelA subunit. *Mol. Cell. Biol.*, **19**, 4798–4805.
53. Takahashi, K., Murakami, M. and Yamanaka, S. (2005) Role of the phosphoinositide 3-kinase pathway in mouse embryonic stem (ES) cells. *Biochem. Soc. Trans.*, **33**, 1522–1525.
54. Vallier, L., Alexander, M. and Pedersen, R.A. (2005) Activin/Nodal and FGF pathways cooperate to maintain pluripotency of human embryonic stem cells. *J. Cell Sci.*, **118**, 4495–4509.
55. Kang, H.B., Kim, J.S. and Kwon, H.J. (2005) Basic fibroblast growth factor activates ERK and induces c-fos in human embryonic stem cell line MizhES1. *Stem Cells Dev.*, **14**, 395–401.
56. Rho, J.Y., Yu, K., Han, J.S., Chae, J.I., Koo, D.B., Yoon, H.S., Moon, S.Y., Lee, K.K. and Han, Y.M. (2005) Transcriptional profiling of the developmentally important signalling pathways in human embryonic stem cells. *Hum. Reprod.*, October 20 [Epub ahead of print].
57. Paling, N.R., Wheadon, H., Bone, H.K. and Welham, M.J. (2004) Regulation of embryonic stem cell self-renewal by phosphoinositide 3-kinase-dependent signaling. *J. Biol. Chem.*, **279**, 48063–48070.
58. Sanchez, M.G., Ruiz-Llorente, L., Sanchez, A.M. and Diaz-Laviada, I. (2003) Activation of phosphoinositide 3-kinase/PKB pathway by CB(1) and CB(2) cannabinoid receptors expressed in prostate PC-3 cells. Involvement in Raf-1 stimulation and NGF induction. *Cell. Signal.*, **15**, 851–859.
59. Matin, M.M., Walsh, J.R., Gokhale, P.J., Draper, J.S., Bahrami, A.R., Morton, I., Moore, H.D. and Andrews, P.W. (2004) Specific knockdown of Oct4 and beta2-microglobulin expression by RNA interference in human embryonic stem cells and embryonic carcinoma cells. *Stem Cells.*, **22**, 659–668.
60. Hyslop, L., Stojkovic, M., Armstrong, L., Walter, T., Stojkovic, P., Przyborski, S., Herbert, M., Murdoch, A., Strachan, T. and Lako, M. (2005) Downregulation of NANOG induces differentiation of human embryonic stem cells to extraembryonic lineages. *Stem Cells*, **23**, 1035–1043.
61. Levenstein, M.E., Ludwig, T.E., Xu, R.H., Llanas, R.A., Vandenheuvel-Kramer, K., Manning, D. and Thomson, J.A. (2006) Basic FGF Support of Human Embryonic Stem Cell Self-Renewal. *Stem Cells*, **24**, 568–574.
62. Ying, Q.L., Nichols, J., Chambers, I. and Smith, A. (2003) BMP induction of Id proteins suppresses differentiation and sustains embryonic stem cell self-renewal in collaboration with STAT3. *Cell*, **115**, 281–292.
63. Dvorak, P., Dvorakova, D., Koskova, S., Vodinska, M., Najvirtova, M., Krekac, D. and Hampl, A. (2005) Expression and potential role of fibroblast growth factor 2 and its receptors in human embryonic stem cells. *Stem Cells*, **23**, 1200–1211.
64. Lim, K.H. and Counter, C.M. (2005) Reduction in the requirement of oncogenic Ras signaling to activation of PI3K/AKT pathway during tumor maintenance. *Cancer Cell*, **8**, 381–392.
65. Wang, Y., Wang, F., Sun, T., Trostinskaia, A., Wygle, D., Puscheck, E. and Rappolee, D.A. (2004) Entire mitogen activated protein kinase (MAPK) pathway is present in preimplantation mouse embryos. *Dev. Dyn.*, **231**, 72–87.
66. Xie, Y., Wang, Y., Sun, T., Wang, F., Trostinskaia, A., Puscheck, E. and Rappolee, D.A. (2005) Six post-implantation lethal knockouts of genes for lipophilic MAPK pathway proteins are expressed in preimplantation mouse embryos and trophoblast stem cells. *Mol. Reprod. Dev.*, **71**, 1–11.
67. Yoshida-Koide, U., Matsuda, T., Saikawa, K., Nakanuma, Y., Yokota, T., Asashima, M. and Koide, H. (2004) Involvement of Ras in extraembryonic endoderm differentiation of embryonic stem cells. *Biochem. Biophys. Res. Commun.*, **313**, 475–481.
68. Tanaka, S., Kunath, T., Hadjantonakis, A.-K., Nagy, A. and Rossant, J. (1998) Promotion of trophoblast stem cell proliferation by FGF4. *Science*, **282**, 2072–2075.
69. Peters, T.J., Chapman, B.M. and Soares, M.J. (2000) Trophoblast differentiation. An *in vitro* model for trophoblast giant cell development. *Methods Mol. Biol.*, **137**, 301–311.
70. Burdon, T., Stracey, C., Chambers, I., Nichols, J. and Smith, A. (1999) Suppression of SHP-2 and ERK signalling promotes self-renewal of mouse embryonic stem cells. *Dev. Biol.*, **210**, 30–43.
71. Qi, X., Li, T.G., Hao, J., Hu, J., Wang, J., Simmons, H., Miura, S., Mishina, Y. and Zhao, G.Q. (2004) BMP4 supports self-renewal of embryonic stem cells by inhibiting mitogen-activated protein kinase pathways. *Proc. Natl Acad. Sci. USA*, **101**, 6027–6032.
72. Lodge, P., McWhir, J., Gallagher, E. and Sang, H. (2005) Increased gp130 signaling in combination with inhibition of the MEK/ERK pathway facilitates embryonic stem cell isolation from normally refractory murine CBA blastocysts. *Cloning Stem Cells*, **7**, 2–7.
73. Takahashi, K., Mitsui, K. and Yamanaka, S. (2003) Role of ERas in promoting tumour-like properties in mouse embryonic stem cells. *Nature*, **423**, 541–545.
74. Takahashi, K., Murakami, M. and Yamanaka, S. (2005) Role of the phosphoinositide 3-kinase pathway in mouse embryonic stem (ES) cells. *Biochem. Soc. Trans.*, **33**, 1522–1525.
75. Wandzioch, E., Edling, C.E., Palmer, R.H., Carlsson, L. and Hallberg, B. (2004) Activation of the MAP kinase pathway by c-Kit is PI-3 kinase dependent in hematopoietic progenitor/stem cell lines. *Blood*, **104**, 51–57.
76. Hu, Q., Klippel, A., Muslin, A.J., Fantl, W.J. and Williams, L.T. (1995) Ras-dependent induction of cellular responses by constitutively active phosphatidylinositol-3 kinase. *Science*, **268**, 100–102.
77. Chou, C.H., Wei, L.H., Kuo, M.L., Huang, Y.J., Lai, K.P., Chen, C.A. and Hsieh, C.Y. (2005) Up-regulation of interleukin-6 in human ovarian cancer cell via a Gi/PI3K-Akt/NF-kappaB pathway by lysophosphatidic acid, an ovarian cancer-activating factor. *Carcinogenesis*, **26**, 45–52.
78. Morel, J., Audo, R., Hahne, M. and Combe, B. (2005) Tumor necrosis factor-related apoptosis-inducing ligand (TRAIL) induces rheumatoid arthritis synovial fibroblast proliferation through mitogen-activated protein kinases and phosphatidylinositol 3-kinase/Akt. *J. Biol. Chem.*, **280**, 15709–15718.
79. Draper, J.S., Smith, K., Gokhale, P., Moore, H.D., Maltby, E., Johnson, J., Meisner, L., Zwaka, T.P., Thomson, J.A. and Andrews, P.W. (2004) Recurrent gain of chromosomes 17q and 12 in cultured human embryonic stem cells. *Nat. Biotechnol.*, **22**, 53–54.
80. Draper, J.S., Moore, H.D., Ruban, L.N., Gokhale, P.J. and Andrews, P.W. (2004) Culture and characterization of human embryonic stem cells. *Stem Cells Dev.*, **13**, 325–336.